CONTACT INFORMATION
Mining Records Curator
Arizona Geological Survey
416 W. Congress St., Suite 100
Tucson, Arizona 85701
602-771-1601
http://www.azgs.az.gov
inquiries@azgs.az.gov

The following file is part of the Grover Heinrichs Mining Collection

ACCESS STATEMENT

These digitized collections are accessible for purposes of education and research. We have indicated what we know about copyright and rights of privacy, publicity, or trademark. Due to the nature of archival collections, we are not always able to identify this information. We are eager to hear from any rights owners, so that we may obtain accurate information. Upon request, we will remove material from public view while we address a rights issue.

CONSTRAINTS STATEMENT

The Arizona Geological Survey does not claim to control all rights for all materials in its collection. These rights include, but are not limited to: copyright, privacy rights, and cultural protection rights. The User hereby assumes all responsibility for obtaining any rights to use the material in excess of "fair use."

The Survey makes no intellectual property claims to the products created by individual authors in the manuscript collections, except when the author deeded those rights to the Survey or when those authors were employed by the State of Arizona and created intellectual products as a function of their official duties. The Survey does maintain property rights to the physical and digital representations of the works.

QUALITY STATEMENT

The Arizona Geological Survey is not responsible for the accuracy of the records, information, or opinions that may be contained in the files. The Survey collects, catalogs, and archives data on mineral properties regardless of its views of the veracity or accuracy of those data.

STATE OF MONTANA
Thomas L. Judge, *Governor*

BUREAU OF MINES AND GEOLOGY
S. L. Groff, *Director*

MEMOIR 43
January 1973

PETROLOGY OF THE NORTHEASTERN BORDER ZONE OF THE IDAHO BATHOLITH, BITTERROOT RANGE, MONTANA

by

Ronald B. Chase

STATE OF MONTANA
BUREAU OF MINES AND GEOLOGY
S. L. Groff, Director

MEMOIR 43

PETROLOGY OF THE NORTHEASTERN BORDER ZONE OF THE IDAHO BATHOLITH, BITTERROOT RANGE, MONTANA

by

Ronald B. Chase
Southern Colorado State College
Pueblo, Colorado

MONTANA COLLEGE OF MINERAL SCIENCE AND TECHNOLOGY
Butte, Montana
1973

Distributed by

Montana Bureau of Mines and Geology

Room 203-B, Main Hall

Montana College of Mineral Science and Technology

Butte, Montana 59701

CONTENTS

	Page
Abstract	1
Introduction	1
General statement and purpose	1
Location and physical setting	2
Previous investigations	2
Present study	2
Acknowledgments	3
Descriptions of metamorphic rocks	3
Quartzofeldspathic gneiss	3
Pelitic schist	3
Concordant pegmatite bodies in quartzofeldspathic and pelitic units	5
Calc-silicate gneiss	5
Amphibolite	5
Anorthosite	5
Metatonalite	5
Descriptions of Idaho batholith and associated igneous rocks	6
Noncataclastic interior	6
Zone of weak cataclasis	8
Zone of strong cataclasis	8
Boundaries between cataclastic zones	9
Biotite schist xenoliths in the Idaho batholith	10
Compositional zonation and petrologic diversity in the batholith contact zone	10
Batholith apophyses, aplite, and pegmatite in adjacent metamorphic rocks	10
Metamorphic conditions	11
Regional metamorphism	11
Possible contact-metamorphic effects	13
Parentage of metamorphic rocks	13
Quartzofeldspathic, pelitic, and calc-silicate units	13
Amphibolite and anorthosite	13
Metatonalite	13
Emplacement of the Idaho batholith	14
Structural analysis	16
Structures in regional metamorphic units	16
Structural surfaces	16
Lineations	16
Mesoscopic folds	16
Transposed layering	17
Structures in cataclastic parts of the Idaho batholith	17
Structural surfaces	17
Lineations	18
Biotite and quartz orientation	18
Structural and metamorphic history	20
Conclusions	21
Possible economic implications	22
References cited	22
Explanation of photographs	24

ILLUSTRATIONS

Plate — Page

1. Geologic map and structure sections of northeastern border of Idaho batholith, Bitterroot Range, Montana . . . . . (in pocket)
2. Photographs of 1) typical pelitic schist, 2) folds in pelitic schist, 3) thin section of pelitic schist, 4) pegmatite in gneiss 25
3. Photographs of 1) calc-silicate gneiss, 2) pegmatite in metatonalite, 3) thin section of granodiorite, 4) thin section of microcline megacryst in batholith rock 26
4. Photographs of 1) quartz monzonite, 2) specimen from batholith showing strong cataclasis, 3) thin section of similar specimen, 4) contact breccia from batholith 27
5. Photographs of 1) contact zone of batholith with gneiss, 2) xenolith in apophysis of batholith, 3) thin section of mineral assemblage A_3, 4) thin section of mineral assemblage A_4 28

Figure

1. Index map showing location of area studied 2
2. Variation diagram, rocks of Idaho batholith and cataclastic equivalents 9
3. ACFK diagram, A_3 and A_4 mineral assemblages 12
4. Probable univarient stability range of paragneissic metamorphic assemblages 13
5. NaCaMg diagram illustrating possible contamination relationship between calc-silicate gneiss and adjacent granitic rocks of the batholith 14
6. Ternary modal compositions of samples from Idaho batholith. 15
7. Sketches of mesoscopic folds in quartzofeldspathic gneiss 17
8. Sketches of mesoscopic folds in pelitic schist 18
9. Schematic representation of F_1, F_2, and F_3 fold phases in quartzofeldspathic gneiss 19

TABLES

Table

1. Average modes of metamorphic units 4
2. Average modes of xenoliths and zones of the Idaho batholith 7
3. Chemical analyses and molecular norms of samples from Idaho batholith 8

PETROLOGY OF THE NORTHEASTERN BORDER ZONE OF THE IDAHO BATHOLITH, BITTERROOT RANGE, MONTANA

By Ronald B. Chase *

ABSTRACT

Pelitic, quartzofeldspathic, and calcareous sediments probably of the Belt Supergroup (Precambrian) have been regionally metamorphosed adjacent to the northeastern border of the Idaho batholith within the Bitterroot Range, Montana. The metasedimentary units comprise lithologically layered schists and gneisses, which contain concordant amphibolite pods and anorthosite bodies. Mineral assemblages are characteristic of sillimanite-potassium feldspar-grade or, locally, sillimanite-muscovite grade metamorphism.

Three phases of synmetamorphic penetrative deformation are recognized. Mica schistosity developed parallel to lithologic layering (probably bedding) during the first (F_1) phase. The second deformation (F_2) resulted in flexural slip folding of F_1 structures and development of mica crinkle lineation (paralleling F_2 fold axes) and incipient axial-plane schistosity. The third deformation (F_3) resulted in superposition of flexural slip folds on F_2 structures in quartzofeldspathic layers and concomitant development of crenulation foliation, axial-plane mica schistosity, and transposition structures, which nearly destroyed the F_2 form surface in pelitic layers. Calc-silicate layers were stretched into boudins during one of the penetrative deformations. Synkinematic igneous activity included the anatectic production of pegmatite veins and the emplacement of a tonalite stock in the quartzofeldspathic metasediments.

Emplacement of Idaho batholith quartz monzonite-granodiorite (texturally and chemically complex in nature) and associated apophyses, pegmatite, and aplite postdates regional metamorphism and structural deformation. Foliation in metasediments dipping under the batholith suggests a floor to the pluton in the area mapped, as does the topographic expression of the contact. Magmatic intrusion involving a complex interplay of forceful injection, magmatic stoping, and contact metasomatism is the probable emplacement mechanism. A macroscopic rotation (F_4) of structural subareas in the metasedimentary rocks adjacent to the batholith represents a possible effect of forceful magmatic injection. Thermal recrystallization of quartz and micas in border-zone gneiss accompanied batholithic emplacement, but the mineral assemblages formed during regional metamorphism were in large part stable in the temperature-pressure field of igneous activity.

A segment of the Idaho batholith along the north-trending eastern front of the Bitterroot Range has been subjected to cataclastic flowage. This deformation (F_5) was dominantly penetrative, resulting in the superposition of quartz and mica subfabrics on the pluton.

INTRODUCTION

GENERAL STATEMENT AND PURPOSE

The Bitterroot Range of western Montana can be divided geologically into two sectors. The northern one-third of the range encompasses regionally metamorphosed anorthosite, amphibolite, and mixed gneiss and schist, which have undergone repeated deformation and intrusion by tabular igneous bodies. The southern two-thirds of the range contains the complexly zoned quartz monzonitic, granodioritic, and tonalitic northeastern part of the Idaho batholith. Cataclastic flowage textures have been superimposed upon predominent paragneiss to the north and batholith to the south along the eastern front of the range.

This complex geology was not disclosed in past reconnaissance investigations. Information gained in this project through detailed mapping and sampling of geologically important areas within the range has been synthesized to produce more definitive results, specifically, the location of the northeastern border of the Idaho batholith, the origin of metamorphism adjacent to the pluton, the evolution and delineation of major structural trends within the metamorphic units and their relationship to the batholith border, and the probable mode of batholithic emplacement within the Bitterroot Range.

*Department of Geology, Southern Colorado State College, Pueblo, Colorado.

LOCATION AND PHYSICAL SETTING

The area studied is in northwestern Ravalli County, Montana, within the Hamilton North, Printz Ridge, Victor, Gash Point, and Saint Joseph Peak 7½-minute quadrangles, and it encompasses approximately 100 square miles (Fig. 1).

The Bitterroot Range rises abruptly westward from the Bitterroot Valley along a remarkably straight north-trending front. The range is deeply incised by numerous east-trending glaciated canyons that head in cirques. Most summit altitudes are 9,000 to 10,000 feet. Throughout the study area the glacial erosion resulted in excellent rock exposure and extreme relief, which is ideal for three-dimensional viewing of large-scale geologic features.

PREVIOUS INVESTIGATIONS

Published investigations of the study area within the Bitterroot Range include a geological reconnaissance of the entire Bitterroot Range (Lindgren, 1904); reconnaissance geology of the Missoula 30-minute quadrangle and adjacent areas, including the northeastern border of the Idaho batholith (Langton, 1935); and reconnaissance geology of the Hamilton 30-minute quadrangle, including part of the Idaho batholith and adjacent metamorphic units (Ross, 1950).

Unpublished investigations of sectors within or adjacent to the study area (Groff, 1954a; Anderson, 1959a; Chase, 1961) describe in detail the geology of individual canyons within the Bitterroot Range. Berg (1964) investigated the petrology of anorthosite bodies in the Bitterroot Range, including one within the map area of this project. Nold (1968) conducted a reconnaissance survey of a large area in Idaho adjacent to the northwest boundary of the study area. Abstracts of these investigations have been published by Anderson (1959), Berg (1965), Chase (1965, 1968), Groff (1954), and Nold (1969).

PRESENT STUDY

Ten months in the summers of 1960, 1962, and 1963 were devoted to field study. An initial reconnaissance investigation of the study area and adjacent parts of the Idaho batholith was conducted to identify lithologic units in previously unmapped terrain. The detailed study employed standard mapping procedures in which field data were recorded on U.S. Forest Service aerial photographs and subsequently transferred to ridge-and-stream strip maps by use of a Vertical Sketchmaster. No adequate topographic base map of the entire study area was then available. A stereographic structural analysis of the regionally metamorphosed units supplied pertinent data contributing to conclusions concerning the structural history of the area.

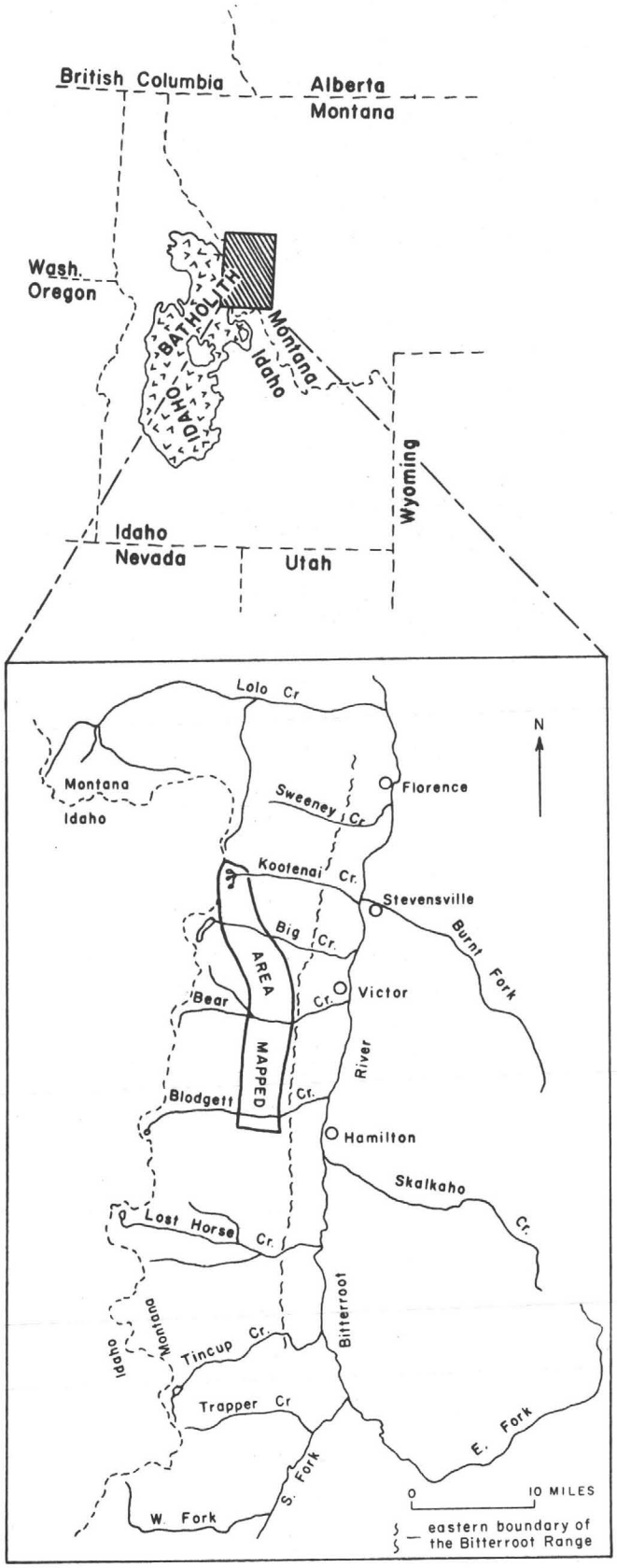

Figure 1.–Index map showing location of area studied.

Specimens (nearly all oriented) collected for structural and petrographic study totaled 1,420, from which 179 thin sections were prepared and carefully examined; 132 of these sections were point counted. Additional laboratory examinations included the x-ray analysis of plagioclase from 12 samples to determine structural state, and whole rock chemical analysis of 12 samples utilizing x-ray fluorescence and flame-photometric techniques.

ACKNOWLEDGMENTS

This investigation was conducted under the supervision of Donald W. Hyndman, Department of Geology, University of Montana, and John Hower, Department of Geology, Case-Western Reserve University. Numerous consultations with Dr. Richard B. Berg during his Bitterroot anorthosite study were extremely helpful in the preparation of this report. The field investigations were financed by National Science Foundation summer fellowships. William Strickler served as field assistant during the summer of 1963. The academic and financial assistance of these contributors is gratefully acknowledged.

DESCRIPTIONS OF METAMORPHIC ROCKS

Regionally metamorphosed rocks bound the Idaho batholith in the northern sector of the map area (Pl. 1). The dominant lithologies are quartzofeldspathic gneiss in contact with the batholith, and pelitic schist (locally gneissic), which is structurally adjacent to and beneath the quartzofeldspathic unit. Both units contain lithologic layers of varying thickness and display schistosity defined by preferred orientation of micas, and both contain amphibolite and calc-silicate gneiss boudins and concordant pegmatite bodies. The schist and gneiss are in sharp parallel contact (with respect to schistosity and layering) and are deformed into mesoscopic similar-, concentric-, and convolute-style folds that produced much structural attenuation. One large tabular anorthosite body is aligned parallel to regional foliation in the pelitic schist. A metamorphosed tonalite stock is mapped in the northwestern sector of the map area. Contacts of tonalite with quartzofeldspathic gneiss are sharp, but biotite schistosity in the tonalite and adjacent gneiss is continuous across the borders.

Average modes for metamorphic units are given in Table 1.

QUARTZOFELDSPATHIC GNEISS

Uniform lithologic layers within the quartzofeldspathic gneiss range in thickness from ¼ to 3½ inches and contain chiefly quartz, feldspar, and biotite in varying proportions, quartz-rich layers being dominant (Pl. 2, fig. 4; Pl. 5, fig. 1). Schistosity is prominent in biotite-rich layers and present also in layers containing minor disseminated biotite. Such schistosity parallels layering in concentric- and (some) similar-style folds, but locally grades from incipient to complete axial-surface schistosity. Composition surfaces of albite twins in plagioclase and of quartz [0001] are not oriented.

Medium-grained interstitial anhedral oligoclase-andesine shows indistinct zoning, albite, albite-Carlsbad, albite-pericline, or albite-Ala B twins, and slight sericitic alteration. Orthoclase and microcline microperthite (locally partly mantled by myrmekitic plagioclase) is fine to medium grained, irregular, and anhedral, and is associated with quartz and mica. Brown biotite is interspersed and contains inclusions of apatite and zircon; local chloritic alteration yields inclusions of sphene, rutile, and opaque minerals. Muscovite generally appears "ragged" and embayed by quartz where acicular clusters of prismatic sillimanite parallel muscovite cleavage flakes. Fine- to medium-grained anhedral quartz showing undulose extinction is interstitial in micaceous and feldspathic layers. Sutured clusters of quartz are common in the more quartzose layers. Grain-to-grain contacts of quartz, muscovite, sillimanite, and potassium feldspar are rare.

PELITIC SCHIST

Throughout the pelitic unit, leucocratic layers ranging in thickness from 1/16 to 3/8 inch and consisting of medium-grained quartz and feldspar alternate with muscovite-sillimanite-biotite layers of similar thickness (Pl. 2, fig. 1). Where the layers are thin, a typical schistose character is present; thicker layers show a banded appearance typical of gneiss. A pronounced schistosity results from strong preferred orientation of biotite and muscovite. In many areas composition layering and schistosity are nearly undistorted except for local folding into the necks of calc-silicate gneiss and pegmatite boudins. This pattern is locally interrupted by similar-style or rootless intrafolial-style folds in which axial surfaces are parallel to schistosity (Pl. 2, fig. 2). Biotite wraps around the apeces of these folds in polygonal arcs (Pl. 2, fig. 3).

Medium-grained oligoclase-endesine is distributed throughout the leucocratic layers and shows albite, pericline, albite-Ala B, and albite-Carlsbad twins, slight sericitization, and virtually no zonation. Some layers

contain occasional large unoriented oligoclase poikiloblasts containing quartz inclusions. Orthoclase microperthite (locally microantiperthitic oligoclase) occurs both in leucocratic layers and in elongate clusters. Fine microperthite grains are intimately mixed with quartz, biotite, muscovite, and sillimanite in micaceous layers. In several specimens, plagioclase adjacent to the potassium feldspar has myrmekitic borders; plagioclase inclusions in the microperthite are mantled with albite. Fine-grained anhedral quartz showing undulose extinction is evenly dispersed through all layers. Coarse sutured quartz grains appear in the elongate feldspathic grain clusters mentioned above. As in the quartzofeldspathic gneiss, biotite, muscovite, and sillimanite do not share grain-to-grain contacts. Most sillimanite forms acicular clusters interstitial to or intergrown with fine- to medium-grained brownish-red biotite, which locally contains inclusions of zircon, apatite, rutile, or opaque minerals. Some small prismatic sillimanite needles are crystallographically oriented within "ragged" (quartz embayed) muscovite. Pink pyralspite garnet and flakes of graphite are interstitial in micaceous layers.

Dispersed layers and pods of hornblende-biotite schist parallel schistosity in the pelitic unit. A typical mode is quartz, 7 percent; bytownite, 9 percent; hornblende, 32 percent; biotite, 52 percent; and accessory apatite. All minerals are medium grained and evenly dispersed (oriented biotite gives strong schistosity) except quartz, which is fine grained and riddles bytownite.

A detailed mesoscopic investigation of the contact of quartzofeldspathic gneiss with pelitic schist reveals (from quartzofeldspathic to pelitic units) an increase in biotite

Table 1.–Average modes of metamorphic units

	1	2	3	4	5	6	7
Unit	Quartzo-feldspathic gneiss	Pelitic schist	Concordant pegmatite bodies	Calc-silicate gneiss	Amphibolite	Anorthosite (Berg, 1964, fig. 7)	Metatonalite
Mineral	(12 analyses)	(8 analyses)	(8 analyses)	(4 analyses)	(2 analyses)	(2 analyses)	(2 analyses)
Quartz	53 (17-83)	38 (31-50)	28 (26-34)	31 (16-45)	17 (14-20)	4 (1-6)	31 (26-37)
Plagioclase	27 (4-68)	12 (4-22)	50 (28-63)	27 (16-37)	12 (11-13)	93 (88-98)	52 (52-52)
Composition of plagioclase	An_{32} (An_{26}-An_{43})	An_{29} (An_{24}-An_{33})	An_{26} (An_{22}-An_{28})	An_{72} (An_{70}-An_{74})	An_{77} (An_{74}-An_{80})	zoned, highly variable average An_{52}	An_{35} (An_{33}-An_{36})
Potassium feldspar	8 (0-28)	11 (3-24)	19 (1-44)				2 (1-4)
Biotite	13 (4-24)	26 (9-46)	5 (1-9)	Tr	5 (2-7)	2 (0-4)	16 (11-19)
Muscovite	1 (0-6)	4 (1-11)	Tr			Tr in 1 sample	Tr
Sillimanite	Tr (0-1)	10 (3-22)					
Hornblende				13 (0-26)	60 (56-64)		Tr
Diopside				29 (16-57)			
Garnet	Tr in 1 sample	Tr in 1 sample		3 (0-8)	3 (0-6)		
Sphene	Tr			Tr (0-1)	Tr		Tr
Opaque minerals excl. graphite	Tr	Tr	Tr		3 (2-3)		Tr
Graphite		Tr in 2 samples					
Myrmekitic plagioclase	Tr	Tr	Tr				Tr
Chlorite	Tr	Tr	Tr	Tr	Tr	1 (1-1)	Tr
Zircon	Tr	Tr	Tr		Tr		Tr
Apatite	Tr	Tr		Tr	Tr		Tr
Clinozoisite						Tr	
Sericite	Tr	Tr	Tr		Tr		Tr
Epidote							Tr
Rutile	Tr	Tr	Tr				Tr

content, a decrease (except locally) in quartz and plagioclase content, the appearance of sillimanite as a major mineral, and a color change from gray to deep red. Interlayering of the two units is present locally, the schistosity and layering in both units being parallel to the contact.

CONCORDANT PEGMATITE BODIES IN QUARTZOFELDSPATHIC AND PELITIC UNITS

Unzoned concordant hypidiomorphic-granular pegmatite bodies 1 inch to several inches thick occur as isolated boudins with sharp borders in the pelitic schist and as continuous layers, which show ptygmatic fold styles and mafic selvages, in the quartzofeldspathic gneiss (Pl. 2, fig. 4).

Medium-grained to coarse-grained oligoclase displays albite twins and no zonation. Potassium feldspar is coarse grained, irregular, and contains string-type microperthitic exsolutions. Quartz occurs as large irregular grains, some of which are composite, and shows undulose extinction. Medium-grained interstitial biotite and muscovite align to give the pegmatite bodies a weak schistosity paralleling contacts. Myrmekitic plagioclase is interstitial to the major minerals. Chlorite, zircon, rutile, sericite, and opaque minerals are alteration products of, or inclusions in, the major minerals.

CALC-SILICATE GNEISS

Numerous pale-green diopsidic calc-silicate boudins 2 by 2 to 4 by 50 feet in planar dimensions occur in the quartzofeldspathic gneiss and pelitic schist. These boudins do not form a distinct regional pattern but tend to be concentrated in the quartzofeldspathic unit, and locally they rim the northeastern border of the Idaho batholith. Alternating composition layers containing plagioclase, hornblende, diopside, and quartz (where present) in varying proportions give the rock a gneissic structure (Pl. 3, fig. 1).

Fine- to coarse-grained quartz, showing slightly undulose extinction, and unzoned bytownite, twinned according to the albite or combined albite-Carlsbad or albite-pericline laws, are concentrated in leucocratic layers. Fine to coarse elongate commonly twinned hornblende grains show subparallelism, imparting a weak lineation in the planes of lithologic layering. Diopside grains are anhedral, elliptical or irregular, and of various sizes. Fine-grained biotite locally accompanies hornblende and is partly altered to chlorite and sphene. Garnet (probably grossularite-rich) occurs as fine anhedral inclusion-free grains in plagioclase or as clusters and strings in diopside-rich layers. Fine-grained apatite and zircon are interstitial.

Contacts between the calc-silicate boudins and host units are sharp. Lithologic layering in boudins generally parallels layering and mica schistosity in the adjacent schist and gneiss, except where host schistosity is warped into the necks of boudins.

AMPHIBOLITE

Lenticular boudins 2 to 3 feet wide and 10 to 50 feet long, consisting of medium-grained amphibolite, parallel the layering and schistosity in the pelitic and quartzofeldspathic units. Contacts are sharp; hornblende lineation parallels the long dimension of the boudins and the foliation surfaces in the surrounding schist and gneiss. Coarse-grained tonalitic lenses and pods, sharply bounded, are sandwiched between most amphibolite boudins and penetrate the hornblende rock.

The hornblende is green, pleochroic, elongate, subhedral, commonly twinned, and slightly chloritized. Bytownite is twinned according to the albite and pericline laws and shows barely visible reverse zoning in some grains. Red garnet (probably almandine-rich), locally chloritized, forms coarse, anhedral poikiloblasts with fractured borders. Rounded quartz showing undulose extinction is interstitial and also occurs as inclusions in plagioclase and garnet (no orientation pattern of inclusions is evident). Some biotite is included in hornblende and garnet, but most cleavage flakes are dispersed and partly oriented in a weak schistosity.

ANORTHOSITE

One large anorthosite body in the study area was mapped and described by Berg (1964). The unit is a massive, hypidiomorphic-granular, tabular body aligned parallel to the regional foliation (including schistosity) of the pelitic schist. Contacts are sharp and associated with concentrations of parallel biotite and chlorite flakes in the anorthosite (schistosity parallels contacts) and concordant amphibolite and quartz monzonitic gneiss layers in the pelitic unit.

Plagioclase (oligoclase to bytownite) shows strong normal or oscillatory zoning and extreme grain-to-grain variation in composition. Most grains are medium size and equant, but megacrysts as large as 7 mm are not uncommon. Twinning is according to the albite, albite-Carlsbad, or albite-pericline laws. Fine-grained quartz showing undulose extinction is interstitial to plagioclase or forms veinlets and inclusions in plagioclase megacrysts. Small flakes of biotite (many of them altered to chlorite) and muscovite are dispersed throughout the anorthosite. Clinozoisite occurs both as fine disseminated grains and as elongate clusters along chlorite cleavages.

METATONALITE

The tonalite occupies an area of 1 square mile within the quartzofeldspathic gneiss and is foliated, medium grained, and allotriomorphic granular in texture. The andesine is subhedral, indistinctly zoned, slightly sericitized,

and contains few inclusions. The dimensional alignment of andesine gives the rock a strong lineation. Twin types are albite, albite-Carlsbad, and albite-pericline. Slightly perthitic potassium feldspar (where present) and interstitial quartz showing undulose extinction are evenly distributed. Biotite commonly occurs in small clusters, which wrap around feldspars, and parallel cleavage flakes define a weak schistosity. Local concentrations of biotite define mesoscopic schlieren structures (Pl. 3, fig. 2). Accessory minerals are generally interspersed.

Veins of pegmatite and aplite, and concordant lenses of quartzofeldspathic gneiss are present in the tonalite. Where pegmatites cross foliation, they either are folded with axial-plane biotite schistosity paralleling that of the host tonalite (Pl. 3, fig. 2), occupy planes of offset in foliation or biotite schlieren, display replacement effects and are bounded in many places by mafic selvages, or demonstrate dilational effects. The replacement veins are rare.

The contact of metatonalite with quartzofeldspathic gneiss is sharp and discordant to layering in the gneiss; schistosity, however, tends to be continuous across the contact. Quartzofeldspathic xenoliths in the tonalite display similar contact relationships, as do tonalite dikes in the gneissic host.

DESCRIPTIONS OF IDAHO BATHOLITH AND ASSOCIATED IGNEOUS ROCKS

The greater part of the study area (southern and western sectors) contains igneous rocks of the Idaho batholith. The pluton is a complex unit, which shows both compositional and textural zonation. The zones were studied in detail, expressed on the geologic map (Pl. 1) where scale permits, and delineated as follows:

1. Noncataclastic interior.—Medium-grained allotriomorphic to hypidiomorphic-granular quartz monzonite, granodiorite, and tonalite (irregular and gradational zonation on small scales) with predominantly isotropic fabric and local quartz-biotite schlieren.

2. Zone of weak cataclasis.—Rock similar to that of the noncataclastic interior but slightly gneissic in appearance where quartz-feldspar crush layers wrap around feldspar augen and where subparallel biotite and muscovite form a weak schistosity.

3. Zone of strong cataclasis.—Rock similar to that of the noncataclastic interior but very gneissic, the quartz and feldspars generally segregated into layers that wrap around feldspar augen; mica schistosity and lineation defined by elongate feldspar augen, composite quartz lenses, and lenses of uncrushed rock are conspicuous.

4. Tonalite-calc-silicate gneiss contact association.—Zone of tonalite and calc-silicate xenoliths, which form a contact breccia along the batholith border.

5. Granodiorite-quartzofeldspathic gneiss contact association.—Zone of granodiorite and quartzofeldspathic xenoliths with gradational boundaries along the batholith border.

6. Batholith apophyses in contact rocks and pegmatite and aplite dikes both within and outside the batholith.

NONCATACLASTIC INTERIOR

Rock composition within the Idaho batholith ranges between that of quartz monzonite and of tonalite, as shown by the modal range (Table 2, col. 1) and chemical compositions (Table 3) of selected samples. A hypidiomorphic-granular texture and isotropic fabric dominate, but some faintly laminated or gneissic zones are outlined by subparallel disseminated biotite (Pl. 3, fig. 3). Contorted foliation patterns in certain areas (not restricted to the border zone) of the pluton are marked by pronounced biotite parallelism, biotite-quartz schlieren, and pegmatitic stringers. These compositional and textural changes are irregular and gradational and can be observed locally in a single outcrop.

The dominant potassium feldspar is microcline microperthite and is distinguished by grid twinning (not observed in all grains) and bead and string-type exsolutions. Large microcline megacrysts are poikilitic and contain many inclusions oriented relative to the crystallographic directions of microcline and some inclusions clustered as multiple-grained rock fragments (Pl. 3, fig. 4 is an example of the latter). Such poikilocrysts give a "porphyritic" texture to portions of the batholith (Pl. 4, fig. 1). In such irregular "porphyritic" zones, the groundmass generally lacks potassium feldspar. Where poikilocrysts are absent, medium-grained microcline and fine-grained untwinned orthoclase occur interstitially, singly, or in mutual association. Oligoclase-andesine shows weak to strong normal zoning, weak oscillatory and reverse zoning, albite, Carlsbad, albite-Ala B, albite-Carlsbad, and albite-pericline twins, and slight sericitic alteration. These grains are small to large in interstitial positions and small as inclusions in the microcline megacrysts. Most plagioclase grains that are peripheral to or included in the microcline megacrysts are mantled by albite at the potassium feldspar interface. Some such plagioclase grains are also myrmekitic. Fine flakes of biotite (most of which are partly altered to chlorite) and muscovite are interstitial to or included in feldspars. Fine rutile needles (sagenitic patterns), sphene, and opaque minerals have formed in highly altered biotite. Unaltered biotite generally contains

Table 2.–Average modes of xenoliths and zones of the Idaho batholith

	1	2	3	4	5	6	7	8
Unit	Noncataclastic interior	Zone of weak cataclasis along Bitterroot Range front	Zone of strong cataclasis along Bitterroot Range front	Biotite schist inclusions in the Idaho batholith	Calc-silicate gneiss inclusions in the Idaho batholith	Tonalitic border with calc-silicate inclusions	Granodioritic border with quartzofeldspathic inclusions	Apophysis in the Kootenai Creek drainage
Mineral	(33 analyses)	(27 analyses)	(13 analyses)	(6 analyses)	(2 analyses)	(5 analyses)	(4 analyses)	(1 analysis)
Quartz	28 (15-42)	30 (23-39)	28 (19-37)	25 (20-29)	23 (22-23)	32 (25-43)	24 (17-33)	33
Plagioclase	42 (27-69)	43 (20-63)	41 (11-57)	44 (32-53)	35 (34-36)	56 (48-59)	46 (38-56)	30
Composition of plagioclase	An_{27} (An_{20}-An_{36})	An_{27} (An_{24}-An_{33})	An_{27} (An_{18}-An_{35})	An_{36} (An_{32}-An_{43})	An_{44} (An_{40}-An_{48})	An_{34} (An_{31}-An_{38})	An_{32} (An_{30}-An_{34})	An_{28}
Potassium feldspar	22 (Tr-49)	14 (0-31)	16 (Tr-56)	2 (0-7)	Tr	1 (Tr-2)	21 (7-36)	32
Biotite	5 (1-16)	8 (1-18)	10 (5-16)	27 (16-38)	Tr	11 (8-16)	9 (8-16)	5
Muscovite	1 (0-7)	2 (0-13)	3 (Tr-9)	Tr		Tr (0-1)	Tr	Tr
Myrmekitic plagioclase	1 (0-3)	3 (0-6)	2 (Tr-7)	Tr			Tr (Tr-1)	Tr
Chlorite	Tr	Tr	Tr	1 (0-4)	Tr	Tr (Tr-1)	Tr	Tr
Opaque minerals	Tr	Tr	Tr	Tr		Tr	Tr (Tr-1)	Tr
Apatite	Tr	Tr	Tr	Tr		Tr	Tr	
Zircon	Tr	Tr	Tr	Tr	Tr	Tr	Tr	Tr
Sericite	Tr	Tr	Tr	Tr		Tr	Tr	Tr
Rutile	Tr	Tr	Tr	Tr		Tr	Tr	Tr
Sphene	Tr	Tr	Tr	Tr	Tr	Tr	Tr	Tr
Epidote	Tr (4 samples)	Tr (1 sample)	Tr (1 sample)			Tr (1 sample)		
Sillimanite	Tr (5 samples)	Tr (4 samples)						
Hornblende					13 (0-25)			
Diopside					30 (19-42)			

zircon and apatite. In several samples "ragged" muscovite is mixed with sillimanite. Epidote is present in narrow, saussurite-filled veins, but a few grains are interstitial.

ZONE OF WEAK CATACLASIS

Idaho batholith rocks in the noncataclastic interior and in the weak cataclastic zone are virtually identical with respect to mineralogy and chemical composition (compare modal analyses of Table 2, col. 1 and 2; also the variation diagram, Fig. 2). Many of the small textural details are identical also. The distinction between the two zones lies solely in the general microscopic and mesoscopic texture and fabric.

Much quartz and feldspar appear in crush layers, which commonly wrap around coarse feldspar and give the rock a slightly gneissic appearance. Subparallel biotite and muscovite form a weak foliation, and plagioclase and potassium feldspar augen (and occasional composite clusters of sutured quartz) are elongated parallel to this foliation. Crush zones in some localities are not oriented.

ZONE OF STRONG CATACLASIS

The portion of the Idaho batholith herein designated the zone of strong cataclasis has been described previously, by Ross (1950, p. 153), as the metasedimentary border-zone gneiss. The mineralogical and chemical similarity of this unit and the noncataclastic interior of the batholith is apparent (compare modal analyses of Table 2, col. 1 and 3; see also the variation diagram, Fig. 2). Such textural details as the potassium feldspar-myrmekitic plagioclase association and the albite mantles on plagioclase adjacent to uncrushed potassium feldspar are preserved, but cataclastic deformation has destroyed the hypidiomorphic texture characteristic of the noncataclastic interior.

Crushed layers containing fine-grained biotite, quartz, and feldspar (many of the layers contain quartz or feldspar exclusively) form subparallel, wavy surfaces, which commonly wrap around lenticular augen of plagioclase and potassium feldspar (Pl. 4, fig. 2). Subparallel granulated biotite and some muscovite flakes and stringers accentuate

Table 3.–Chemical analyses and molecular norms of samples from Idaho batholith

	Samples from the non-cataclastic interior of the Idaho batholith									Samples from the zone of weak cataclasis		Samples from the zone of strong cataclasis
SiO_2	68.6	67.4	68.3	69.1	73.5	69.0	67.3	63.3	63.3	70.2	70.6	67.7
TiO_2	0.2	0.2	0.2	0.2	0.2	0.2	0.4	0.4	0.6	0.2	0.2	0.2
Al_2O_3	15.3	14.4	14.8	14.8	16.1	14.8	15.2	16.6	16.7	15.3	14.4	15.2
Fe_2O_3	2.4	2.1	2.0	1.3	1.9	2.2	2.8	4.2	5.3	1.6	1.7	2.0
MgO	0.8	0.8	1.0	0.6	0.7	0.7	1.5	1.7	1.5	0.9	0.9	1.5
CaO	1.7	2.0	2.0	1.5	1.8	1.7	3.2	3.5	2.8	1.7	1.6	1.8
Na_2O	4.7	4.8	4.7	3.9	4.7	4.1	4.4	5.4	4.7	3.7	4.6	3.5
K_2O	3.9	3.2	3.5	5.1	4.6	4.5	1.7	1.6	4.3	4.1	4.1	3.6
H_2O^+	0.3	0.5	0.3	0.2	0.3	0.2	0.6	0.3	0.3	0.2	0.3	0.5
TOTAL	97.9	96.4	96.8	96.7	103.8	97.4	97.1	97.0	99.5	97.9	98.4	96.0
	Molecular norms											
q	20.3	21.1	21.2	21.6	21.1	20.8	25.3	15.4	11.0	27.0	22.6	26.8
or	23.5	26.0	21.0	31.5	26.0	28.0	10.5	9.5	25.5	25.0	24.5	22.5
ab	43.5	41.0	43.5	36.5	41.0	39.0	41.0	49.5	42.5	33.5	42.0	33.0
an	8.5	8.5	9.5	7.5	8.5	8.5	16.0	17.0	11.8	8.5	6.8	9.0
c	0.3	0.2	–	0.1	0.2	–	0.5	–	–	2.1	–	2.7
wo	–	–	0.4	–	–	–	–	0.4	0.8	–	0.4	–
en	2.2	1.8	2.8	1.8	1.8	2.0	4.4	5.0	4.2	2.6	2.4	4.4
fs	iron calculated as Fe_2O_3											
il*	0.2	0.2	0.4	0.2	0.2	0.4	0.4	0.6	1.0	0.2	0.2	0.2
mt	iron calculated as Fe_2O_3											
hm	1.6	1.2	1.2	0.8	1.2	1.4	1.8	2.5	3.2	1.0	1.1	1.4
TOTAL	100.1	100.0	100.0	100.0	100.0	100.1	99.9	99.9	100.0	99.9	100.0	100.0

*Sufficient Fe_2O_3 recalculated as FeO to make ilmenite.

the foliation of the crushed layers. Such foliation is locally offset by microfaults (Pl. 4, fig. 3). A weak lineation, within foliation planes, results from alignment of lenticular augen, mica clusters, and composite quartz lenses. The crush layering, mica foliation, and closely spaced jointing parallel to layering give the unit a uniform east-dipping stratified aspect.

BOUNDARIES BETWEEN CATACLASTIC ZONES

Boundaries between textural zones of the Idaho batholith (Pl. 1) are gradational over a distance of approximately 400 feet. The dominantly isotropic interior of the pluton grades eastward and structurally upward into the zone of weak cataclasis through an alternating sequence of granulated layers and isotropic layers. A gradual but

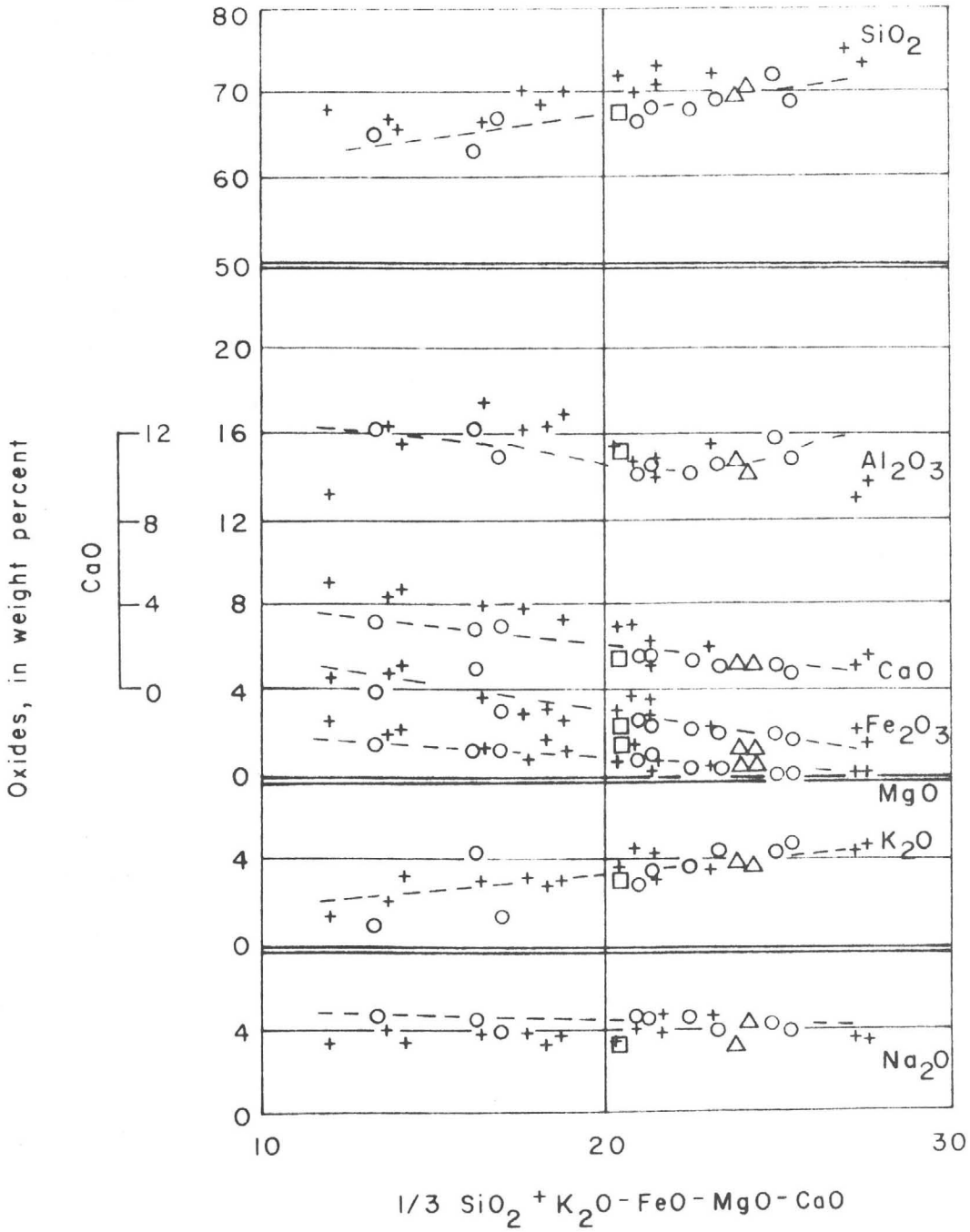

Figure 2.–Variation diagram of Idaho batholith and cataclastic equivalents. Circles–isotropic batholith; triangles–zone of weak cataclasis; squares–zone of strong cataclasis; crosses–Idaho batholith analyses, from Larsen and Schmidt (1958, Fig. 1, where iron is analyzed as FeO). Curves of best visual fit drawn through analyses of rocks from study area.

pronounced increase in the degree of cataclasis and a segregation of quartz into lenses and layers mark the boundary between the zones of weak and strong cataclasis.

BIOTITE SCHIST XENOLITHS IN THE IDAHO BATHOLITH

Layers and pods (xenoliths) of fine-grained biotite schist occur at widely-spaced intervals in the batholith and its cataclastic equivalents. The pods display folded biotite schistosity and contain intrusive pegmatite veins and fingers of host rock. Folded and nonfolded layers are dispersed throughout the pluton but are especially conspicuous in the cataclastic units. Folded layers show Gleitbrett-style structures with respect to foliation in the cataclastic hosts; nonfolded layers parallel this foliation. Schistosity in the biotite schist generally parallels the contacts, but local truncation is not uncommon.

The average mode and modal range of the biotite schist xenoliths is given in Table 2 (col. 4). The plagioclase (andesine) is irregular to equant in shape, has barely visible to moderate zonation, and displays albite, albite-Carlsbad, or albite-pericline twins. Orthoclase is present locally. Equant or irregular quartz occurs interstitially or as inclusions in feldspars. Subparallel flakes of biotite (and muscovite, where present) are distributed evenly throughout the rock. Biotite along the edges of microfractures is altered to chlorite. All accessory minerals (except muscovite) occur as inclusions in the major minerals.

COMPOSITIONAL ZONATION AND PETROLOGIC DIVERSITY IN THE BATHOLITH CONTACT ZONES

The batholith in contact with quartzofeldspathic and calc-silicate gneiss can be macroscopically pictured as a series of sillform granitic bodies, which are marginal to the main massif. There is no precise contact between the batholith and adjacent gneiss. The contact line traced on the geologic map (Pl. 1) represents the position at which the first continuous layers are encountered when traversing into the host rock. Xenoliths of quartzofeldspathic, quartzitic, and calc-silicate rock are numerous adjacent to the contact but sparser toward the interior of the batholith. Near the contact, the trace of schistosity in most xenoliths parallels foliation in the adjacent country rock. Xenoliths farther from the contact zone display no uniform orientation. Calc-silicate or quartzitic xenoliths retain sharp borders, but many of the quartzofeldspathic xenoliths assume "ghostlike" forms, which are outlined by biotite schlieren. Where biotite foliation is clearly recognizable in the pluton, it tends to wrap around the xenoliths.

Where the batholith is rimmed by a mappable zone of calc-silicate rock (Ibc_1, on Pl. 1), inclusions are so abundant that the border zone resembles a contact breccia (Pl. 4, fig. 4). The xenoliths typically show hornblende selvages, and plagioclase composition in the xenoliths is more sodic than that in the calc-silicate gneiss away from the contact zone (andesine instead of bytownite). The batholith in these zones is conspicuously tonalitic (compare average modes in Table 2, col. 5, and Table 1, col. 3; also, Table 2, col. 6 and 1).

In areas designated Ibc_2 on Plate 1, the batholith is in contact with quartzofeldspathic gneiss. Here the contact tends to be gradational, and biotite-rich folia in the gneiss are associated with a granitic matrix. Mesoscopic structures characteristic of the quartzofeldspathic gneiss tend to be undisturbed. Sill-like sheets of isotropic granitic rock (containing zoned plagioclase) ranging in thickness from an inch or less to 100 feet separate the biotite-rich folia (Pl. 5, fig. 1). Although such contacts tend to be gradational and generally concordant on the mesoscopic scale, in some areas the lithologic layering and schistosity in the gneissic layers are truncated by granitic material, and no "ghostlike" gneissic remnants continue into the igneous rock. The batholith in these zones is conspicuously granodioritic (compare average modes in Table 2, col. 7 and 1).

BATHOLITH APOPHYSES, APLITE, AND PEGMATITE IN ADJACENT METAMORPHIC ROCKS

Numerous dikelike apophyses of quartz monzonite and granodiorite protrude from the main batholithic body and truncate the schistosity in the quartzofeldspathic, pelitic, and metatonalitic units (Pl. 5, fig. 2). A few such apophyses can be traced directly into the host gneisses for short distances. Where such apophyses cannot be traced directly into the batholith at the presently exposed level, mineralogical, modal, and textural correlations (including the presence of potassium feldspar megacrysts in many dikes) indicate derivation from the batholith. Concordant pegmatite bodies in the gneiss are truncated by the batholith. Pegmatite and aplite veins, which form a complex network in the batholith margin, penetrate locally into the host rocks, crosscutting the earlier formed metamorphic pegmatite bodies.

METAMORPHIC CONDITIONS

REGIONAL METAMORPHISM

The following mineral assemblages occur in quartzofeldspathic, pelitic, and calc-silicate gneiss and amphibolite:

A_3 – Sillimanite-muscovite-grade metamorphism
(1) biotite-quartz-plagioclase (An_{25-43})-muscovite-(± sillimanite)-(± orthoclase)-(± almandine)

A_4 – Sillimanite-potassium feldspar-grade metamorphism
(2) quartz-biotite-plagioclase (An_{24-34})-orthoclase (locally microcline)-sillimanite-muscovite-(± almandine)

A_3 or A_4
(3) quartz-biotite-plagioclase (An_{31-35})-(± orthoclase)
(4) hornblende-quartz-plagioclase (An_{71-80})-biotite-(± sphene)-(± almandine)
(5) hornblende-plagioclase (An_{72-74})-(± quartz)-diopside-(± biotite)-sphene
(6) quartz-plagioclase (An_{70-72})-diopside-grossularite-sphene

ACFK diagrams for each assemblage are given in Figure 3. Zircon, opaque minerals (locally graphite in the pelitic schist), and myrmekitic plagioclase are present in trace quantities. Slightly chloritized biotite (containing sagenitic rutile) and sericitized plagioclase are the result of retrograde changes.

The basis for subdivision of sillimanite-orthoclase-bearing assemblages into A_3 and A_4 is strictly textural. In A_3 assemblages, muscovite is a minor mineral and coexists with variable quantities of medium- to coarse-grained orthoclase in quartz-feldspar lenses. The muscovite is in the form of "clean" grains with smooth, sharp borders and is locally not in contact with orthoclase. Sillimanite is commonly located along the borders of "clean" biotite grains associated with muscovite and polygonal quartz in micaceous layers (Pl. 5, fig. 3). In A_4 assemblages, muscovite (locally fibrolite-bearing) occurs in trace quantities along with variable quantities of interstitial orthoclase. The muscovite grains display ragged borders and appear to be corroded in the presence of quartz. Orthoclase and sillimanite are locally but not everywhere associated with muscovite. Sillimanite appears to be replacing, or forming epitaxial growths on, biotite grains, but other biotite grains are relatively "clean" (Pl. 5, fig. 4).

The above textural evidence suggests disequilibrium and leads to the conclusion that the "clean" muscovite (and not orthoclase) was stable in the presence of quartz below the temperature of the reaction

$$\text{muscovite} + \text{quartz} \rightleftharpoons \text{sillimanite} + \text{orthoclase} + H_2O$$

during the maximum temperature of metamorphism. The presence of "ragged" muscovite texturally associated with quartz indicates a metamorphic temperature conducive to this reaction in the incipient stage. Guidotti (1963) and Evans and Guidotti (1966), however, have shown the possibility that these minerals can coexist in chemical equilibrium, arising through the reaction

$$\text{muscovite} + \text{quartz} + \text{Na-plagioclase} \rightleftharpoons \text{sillimanite} + \text{Na-orthoclase} + \text{more calcic plagioclase} + H_2O$$

A test of equilibrium under these chemical conditions would require detailed chemical analyses of numerous rock samples and corresponding analyses of each critical mineral phase, a study beyond the scope of the present project.

The temperature and pressure (P_{H_2O}) conditions necessary to produce the above mineral assemblages can be tentatively predicted on the basis of experimentally established univarient stability curves for minerals present in the assemblages. These critical univarient curves, given in Figure 4, are:

(A) Muscovite + quartz ⇌ sillimanite + orthoclase + H_2O (Weill, 1966, Fig. 5, with extrapolation to P_{H_2O} above 2kb). This curve could shift slightly from its plotted position with variation in impurities or X_{H_2O} in the natural rocks.

(B) Muscovite ⇌ sanidine + corundum + H_2O (Velde, 1965, Fig. 1). This reaction places an upper temperature limit on the stability of muscovite.

(C) Kyanite ⇌ sillimanite (Newton, 1966, p. 171).

(D) Cordierite + Fe-biotite ⇌ almandine + Mg-biotite + Al_2SiO_5 + H_2O (data by Hirschberg, *in* Winkler, 1965, p. 160). Applicability of this reaction is suspect because the composition of almandine in the pelitic and quartzofeldspathic units is unknown, and the composition of synthetic cordierite in the experimental runs was not reported.

(E) The upper pressure stability limit of cordierite as estimated on the basis of petrographic considerations (Hyndman, 1967, personal communication).

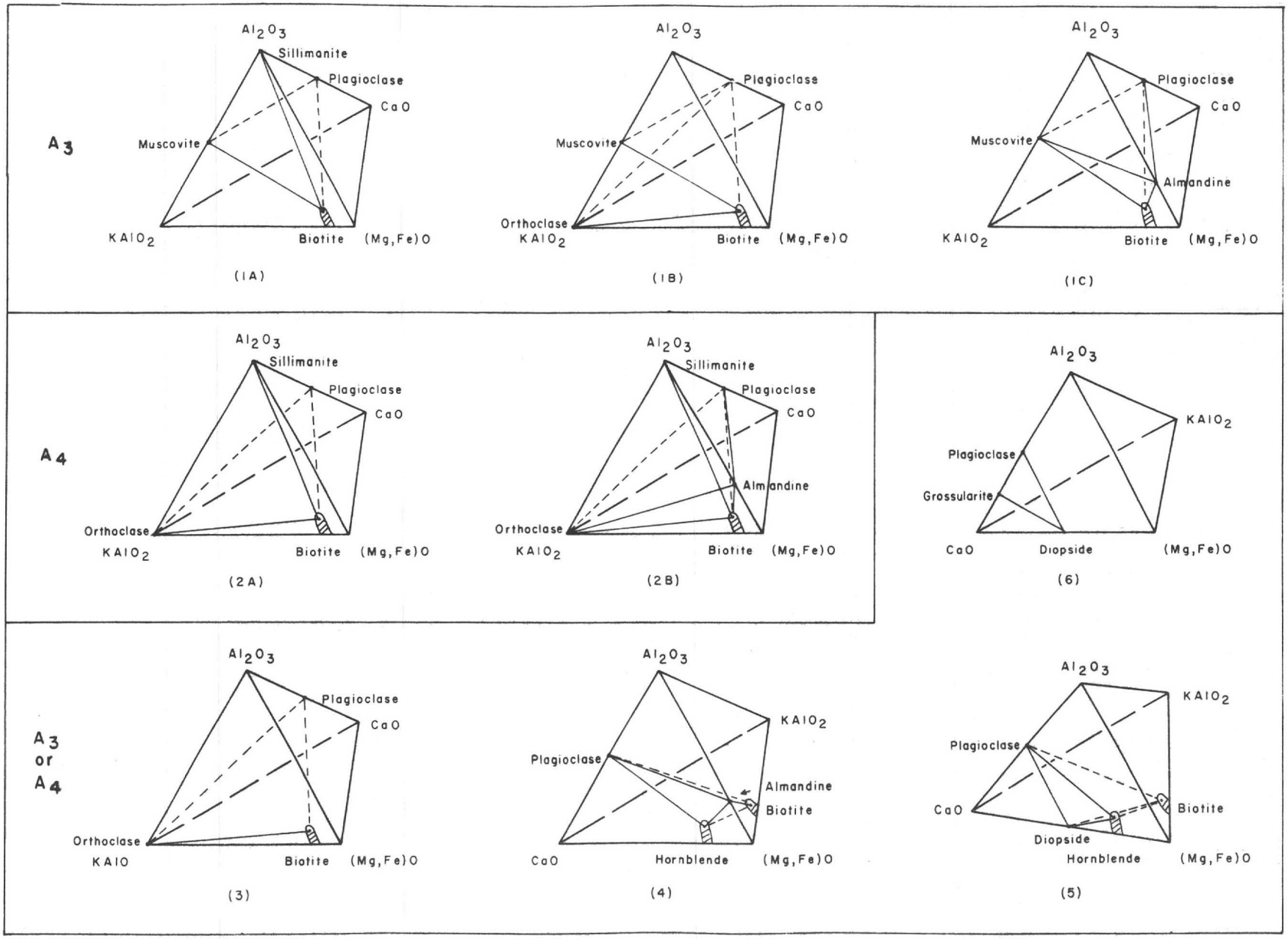

Figure 3.–ACFK diagrams for A_3 (sillimanite-muscovite-grade) and A_4 (sillimanite-potassium feldspar-grade) assemblages. All assemblages, except local calc-sillicate assemblages (5), also contain quartz.

In view of the above considerations, a tentative metamorphic temperature of about 675°C and P_{H_2O} of about 6kb can be predicted. Such conditions are conducive to anatexis in the metamorphic units to produce pegmatite mobilizates, which crystallize *in situ* leaving mafic selvages in adjacent gneiss, or migrate to lower pressure-temperature regions within the metamorphic units (Winkler, 1965, p. 199-203; von Platen, 1965, p. 203-218).

POSSIBLE CONTACT-METAMORPHIC EFFECTS

Some hydrothermal epidote occurs along fractures in the calc-silicate gneiss, but all minerals formed during the period of major regional metamorphism were stable in the temperature-pressure field of batholithic intrusion. Biotite in crenulations within the paragneiss adjacent to the batholith is not bent (Pl. 2, fig. 3), and quartz displays no preferred orientation. Bent mica and oriented quartz are common, however, in similar units away from the contact zone. It is probable that a thermal effect associated with batholithic intrusion produced the recrystallization of mica and quartz within, and limited to, regional metamorphic units of the Idaho batholith border zone.

PARENTAGE OF METAMORPHIC ROCKS

QUARTZOFELDSPATHIC, PELITIC, AND CALC-SILICATE UNITS

The quartz content of the quartzofeldspathic gneiss (53 percent average; 17-83 percent range) and the biotite-plus-sillimanite content of the pelitic schist (26 percent average; 9-46 percent range for biotite; 10 percent average, 3-22 percent range for sillimanite) demonstrate the paragneissic character of these units. The calc-silicate gneiss probably represents a metamorphosed siliceous carbonate within this sequence.

Both paragneisses resemble metamorphosed equivalents of the Prichard Formation of the Belt Supergroup (Precambrian). The Prichard Formation has been described by Ross (1963, p. 58), Hobbs and others (1965), and Gibson (1948, p. 10). The fine layering, intermixed pelitic and quartzofeldspathic composition of the units, and local occurrence of calc-silicate rocks extend into the northern Bitterroot Range where Wehrenberg (1968, p. 456) made a similar correlation. In his stratigraphic study of Belt units and metamorphic equivalents northeast of the Idaho batholith in Idaho, Nold (1968) recognized Prichard Formation metamorphic rocks in the northern sector of the area of this project.

AMPHIBOLITE AND ANORTHOSITE

The amphibolite and anorthosite bodies in the northern Bitterroot Range were described in detail by Berg (1964), who suggested (p. 134) that the amphibolite boudins are metamorphosed and segmented diabase sills or dikes. Those boudins studied in this project give some credence to Berg's suggestion in that almandine (present in most boudins) exists in conjunction with some biotite, opaque minerals are present in more than trace quantities, the quartz content is relatively low, the hornblende/quartz + biotite ratio is high, and lithologic layering is generally absent.

The anorthosite bodies in Big Creek Canyon were not studied for this report. The origin of these bodies was discussed in detail by Berg (1964).

METATONALITE

The metamorphic and orthogneissic character of the metatonalite can be demonstrated by the following: The tonalitic modes and relatively uniform distribution of individual mineral phases, the lithologic discordance of the contact of tonalite with quartzofeldspathic gneiss, the continuity of biotite schistosity across the contact, and the axial-plane biotite schistosity in folded pegmatite bodies, which parallels schistosity in the tonalite body.

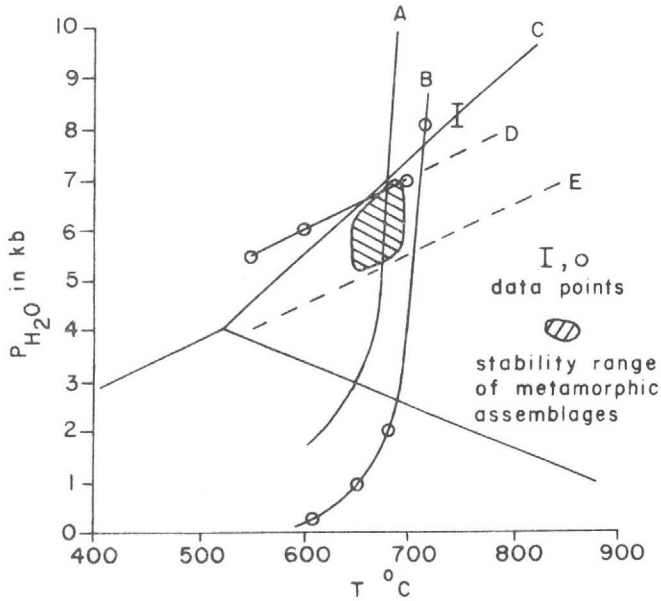

Figure 4.–Probable univarient stability range of paragneissic metamorphic assemblages. See text for explanation.

EMPLACEMENT OF THE IDAHO BATHOLITH

The compositional and textural complexity of the Idaho batholith, excluding the cataclastic zones, seems to be most adequately explained by magmatic emplacement. Batholith apophyses (granitic dikes) display sharp contacts with host paragneiss. The outer margin of the batholith is locally in sharp contact with and discordant to the schistosity and lithologic layering in the host gneiss. Inclusions of biotite-rich or plagioclase-poor quartzofeldspathic gneiss and calc-silicate gneiss are sharply bounded on all sides by granitic material. Biotite foliation, where present in the pluton, wraps around such inclusions. Plagioclase in some marginal and interior parts of the batholith displays normal, reverse, and oscillatory zoning, but the difference in composition between core and rim does not exceed 6 percent An.

Magmatic origin might be questioned on the basis of local gradational contacts with quartzofeldspathic gneiss where metamorphic structures appear undisturbed in a granitic matrix. The local presence of gneissic layers and biotite folia in the predominantly massive interior part of the batholith, the tendency toward structural parallelism of xenoliths close to the batholith contact, and the local presence of sillimanite in the pluton might also raise doubts.

It is no coincidence that the area exhibiting the most gradational contact between the pluton and quartzofeldspathic gneiss is virtually devoid of calc-silicate rock. The chemical contrast between quartz monzonite-granodiorite of the batholith and quartzofeldspathic gneiss is probably sufficiently small that endomorphic reactions between encroaching magma and gneiss could "smooth out" the small concentration gradients, provided a relatively high temperature (eutectic temperature?) and intergranular fluids in the system persisted over a reasonable span of time. Furthermore, the quartz- and feldspar-rich layers in the gneiss would be most susceptible to alkali exchange reactions or to simple recrystallization to produce a granitic texture. (See the discussion of experimental metasomatism by Orville, 1962, 1963.) If the large granitic sills in the gradational contact areas represent magmatic bodies, as the zoned plagioclase in these sills would indicate, they could serve as the source of the marginal granitizing agents. Because of extreme chemical differences, quartz- and mica-rich layers and calc-silicate boudins in the adjacent gneiss were preserved.

The spatial association of tonalite and calc-silicate gneiss indicates a chemical relationship suggestive of contamination. Possible reaction trends (without benefit of chemical analyses) are explored in the CaO-MgO-$NaO_{1/2}$ diagram (Fig. 5). A weak linear composition trend between calc-silicate gneiss of variable composition and batholithic rocks is indicated. Certainly, the presence of hornblende on the borders of calc-silicate inclusions is

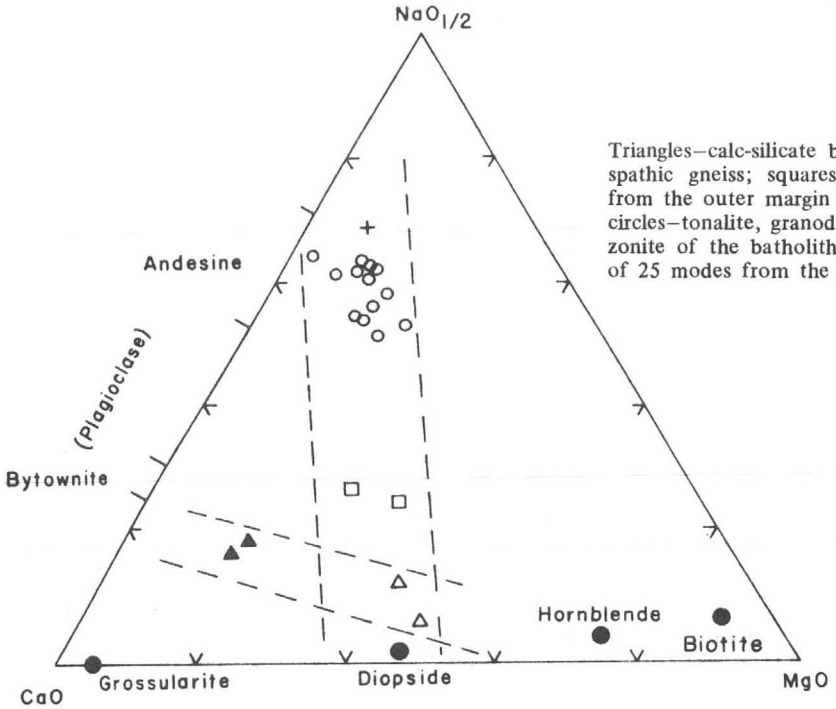

Triangles–calc-silicate boudins in quartzofeldspathic gneiss; squares–calc-silicate xenoliths from the outer margin of the batholith; open circles–tonalite, granodiorite, and quartz monzonite of the batholith margin; cross–average of 25 modes from the batholith interior.

Figure 5.–NaCaMg diagram illustrating possible contamination relationships between calc-silicate gneiss and adjacent granitic rocks of the Idaho batholith. Chemical compositions calculated from modal analysis data. Mineral compositions (closed circles) are from Deer, Howie, and Zussman as follows: grossularite (1962a, Table 16, analysis 3), diopside (1963, Table 5, average of analyses 3, 4, 7), hornblende (1963, Table 40, analysis 1), biotite (1962b, Table 12, average of analyses 3, 6, 7, 9).

suggestive of very local contamination. The minor development of hornblende and the lack of potassium feldspar or biotite in calc-silicate inclusions preclude the loss of significant quantities of potassium from the granitic material. (Hyndman and others, 1968, illustrated the lack of potassium mobility in metamorphosed calc-silicate rock.) The addition of Ca, Mg, and Al to the granitic material could, however, lead to the development of biotite and andesine at the expense of alkali feldspar. Similar statements might apply to granodioritic contact zonation in association with quartzofeldspathic gneiss or irregular zonation in the interior part of the pluton in association with digested gneissic xenoliths, but documentation is lacking at the present stage of investigation.

Modes of noncataclastic batholith rocks are plotted on the ternary composition diagram (Fig. 6). Anatexis under conditions of sillimanite-orthoclase-grade metamorphism or higher is a conceivable origin of the magmatic material associated with the batholith within the study area; most composition points lie close to or on the appropriate cotectic lines of the ternary diagram. The composition spread from quartz monzonite to tonalite could be attributed to contamination effects (see above).

Matrix fragments and concentrically oriented inclusions in potassium feldspar megacrysts are indicative of solid-state growth of the megacrysts. Inclusions in many megacrysts consist of nearly every major mineral and most accessory minerals present in the granitic matrix. The potassium feldspar, being the last major mineral to appear in the paragenetic sequence of granitic rocks (Fig. 6), could have been remobilized locally in areas of pronounced pegmatitic activity during the final stage of magmatic consolidation or later, and thus could replace earlier formed matrix minerals. (An identical conclusion, based on similar textures in the Albtal granite of Germany, has been presented by Emmermann, 1969, p. 294.) Additional subsolidus chemical adjustments included the metasomatic development of myrmekitic plagioclase in the plagioclase adjacent to the potassium feldspar interface, and (as illustrated by Tuttle, 1952, p. 115) subsolidus exsolution of albite from the potassium feldspar lattice with development of albite rims on plagioclase inclusions in such potassium feldspar.

The schistosity in quartzofeldspathic gneiss adjacent to the batholith is nearly everywhere conformable to the border of the pluton; the general dip of this schistosity is under the batholith except in a small area adjacent to the Idaho-Montana boundary. In the north-facing cirques of Big Creek Canyon, granitic rocks of the batholith form the aretes, and topographically lower paragneiss, which has a regional dip of 40° SW, can be traced beneath the batholith for as much as half a mile. No continuous layers of paragneiss were observed in upper Sweathouse Creek Canyon. The structural and topographic expres-

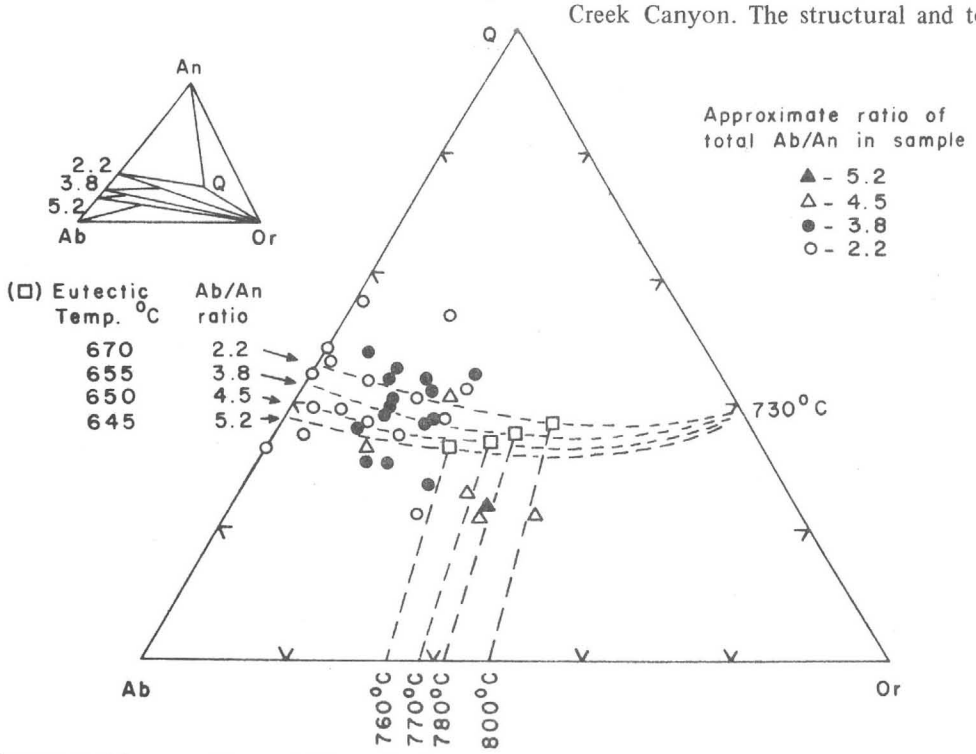

Figure 6.–Ternary modal compositions of 37 samples from the Idaho batholith. Ternary phase diagram is a composite from Winkler (1965, Fig. 34 and 36, Table 10, p. 195) extrapolated to 6kb from data in Tuttle and Bowen (1958, Fig. 22-25), Luth and others (1964, Fig. 2 and 3), and Yoder and others (1957, Fig. 41). Compositions are adjusted to account for limited albite solid solution in the potassium feldspar phase at 675°C (Barth, 1956, Fig. 1). See text for further explanation.

sions of the batholith contact are suggestive of the base of a large granitic sheet. Where paragneiss dips vertically or away from the batholith at a steep angle in the high country near the Idaho-Montana border, the side of the pluton is exposed. It is not known whether this sheetlike expression of the batholith represents a large-scale lateral migration of magma, a marginal digitation on an otherwise steep-walled batholith, or structural rotation of sufficient magnitude to account for a 40° dip of the contact south of Big Creek. No thrust-fault displacement is evident in the contact zone. It is indeed possible that the batholith border is spatially controlled by the calc-silicate rim, which bounds roughly two-thirds of the pluton in the area studied.

STRUCTURAL ANALYSIS

STRUCTURES IN REGIONAL METAMORPHIC UNITS

STRUCTURAL SURFACES

Layering (S_0) in the quartzofeldspathic and pelitic units derives from alternating quartz-feldspar and biotite-muscovite-(± sillimanite) concentrations (Pl. 2, fig. 1, 4). In calc-silicate gneiss, quartz-bytownite and hornblende-diopside layers predominate (Pl. 3, fig. 1). Such layers in these units range from 0.6 and 3.5 inches in thickness and parallel major lithologic contacts. These layers probably represent original sedimentary beds, perhaps compositionally modified by metamorphic differentiation. In metatonalite, local biotite schlieren form discontinuous layers (Pl. 3, fig. 2).

Schistosity (S_1 parallel to lithologic layering, S_2 in axial planar orientation) in quartzofeldspathic and pelitic units is defined by parallelism of biotite and muscovite cleavages and by biotite cleavages in metatonalite. Parallelism of biotite and hornblende imparts schistosity to calc-silicate gneiss and amphibolite.

Crenulation foliation (strain-slip cleavage) (S_2 in axial planar orientation) in the quartzofeldspathic and pelitic units is defined by axial planes of crenulations in micaceous layers, which are parasitic to mesoscopic folds (Fig. 7, 8).

Other structural surfaces include *axial surfaces* of mesoscopic folds (S_2), *pegmatite contacts*, and *joints*.

LINEATIONS

Mineral parallelism is present in the quartzofeldspathic and pelitic units (sillimanite), amphibolite (hornblende), and metatonalite (plagioclase).

Crinkle lineation (L) is defined by open crinkles on micaceous layering surfaces in quartzofeldspathic and pelitic units. Open crinkles and tight crenulations are not equivalent features.

Intersections of layering and schistosity are present where mesoscopic folds show axial-surface schistosity (poorly developed in much of the study area).

Other lineations include *boudinage*, where stretched layers of pegmatite, calc-silicate gneiss, and amphibolite exist in quartzofeldspathic and pelitic units, and *axes* or *hinges* of mesoscopic folds (B_1 and B_2).

MESOSCOPIC FOLDS*

Concentric-style folds show uniform curvature and poorly defined hinge lines (Fig. 7a, 7b, and part of 7c). Schistosity (S_1) generally conforms to curvature in folded layers. Local axial-surface schistosity and crenulation foliation (S_2 for both surfaces) are present (Fig. 7f) in association with some thickening and thinning of layers. Crinkle lineations (L) parallel axes of some concentric-style folds (B_1) and diverge from the axes in small-circle girdle patterns in other such folds, a result of multiple deformation (Fig. 9). Concentric-style folds are common in the quartzofeldspathic gneiss and present locally in pelitic schist (Pl. 2, fig. 1).

Tight, isoclinal, *similar-style* folds having well defined hinge lines are commonest in pelitic schist (Fig. 8) but are present locally in micaceous layers of the quartzofeldspathic gneiss (Fig. 7c, 7d, and 7e). Axes of such folds plot in great-circle patterns, a result of multiple deformation (Fig. 9). Axial-surface schistosity and crenulation foliation are common (Fig. 7h, 8); schistosity conforms to layering in some folds (Fig. 7c, 7d, and 7e). Attenuation of fold limbs is common in pelitic schist (Fig. 8).

Within the quartzofeldspathic gneiss, groups of small-scale similar- and concentric-style folds (wave length of 1 inch or less) are associated in *convolute-style* patterns (Fig. 7g).

*Classification according to Turner and Weiss, 1963, p. 106-117. The terms *microscopic* and *mesoscopic* are derived from the Greek roots for *small* and *intermediate*. The proper correlative term would be *megascopic*, from the Greek root for *large*, but some authors prefer *macroscopic*, from the Latin root for *wide* or *broad*.

Rootless-intrafolial-style folds consist of doubly attenuated similar-style folds, which appear as tectonic inclusions in relatively unfolded parts of the pelitic schist (Fig. 8a). Quartzofeldspathic layers and hornblende-biotite layers typically form such folds. Axial surfaces (S_2) of these folds approximately parallel schistosity (S_1) in adjacent rock.

Concordant pegmatite layers in the quartzofeldspathic gneiss display *ptygmatic-style* patterns. Mafic selvages commonly outline such pegmatite bodies (Pl. 2, fig. 4).

TRANSPOSED LAYERING

In the pelitic schist, transposition is indicated on the outcrop scale by attenuated limbs in folded quartzofeldspathic, mafic, and pelitic layers (Fig. 8). Transposition can also be seen in thin section where sillimanite outlines ghostlike crenulations with biotite cleavages in axial-planar orientation. Such transposed layers are prevalent in appressed, similar-style folds where reoriented layering parallels fold limbs.

STRUCTURES IN CATACLASTIC PARTS OF THE IDAHO BATHOLITH

STRUCTURAL SURFACES

Crushed layers containing fine-grained mosaics of biotite, quartz, and feldspar (in many places segregated), and biotite foliation parallel to these layers form the obvious mesoscopic foliation (Pl. 4, fig. 2, 3). Such foliation also occurs locally, but in zones too small and irregular to be delineated on Plate 1, in that area designated as the noncataclastic interior of the batholith.

Biotite schist and pegmatite *contact surfaces* generally parallel foliation in cataclastic sections of the batholith,

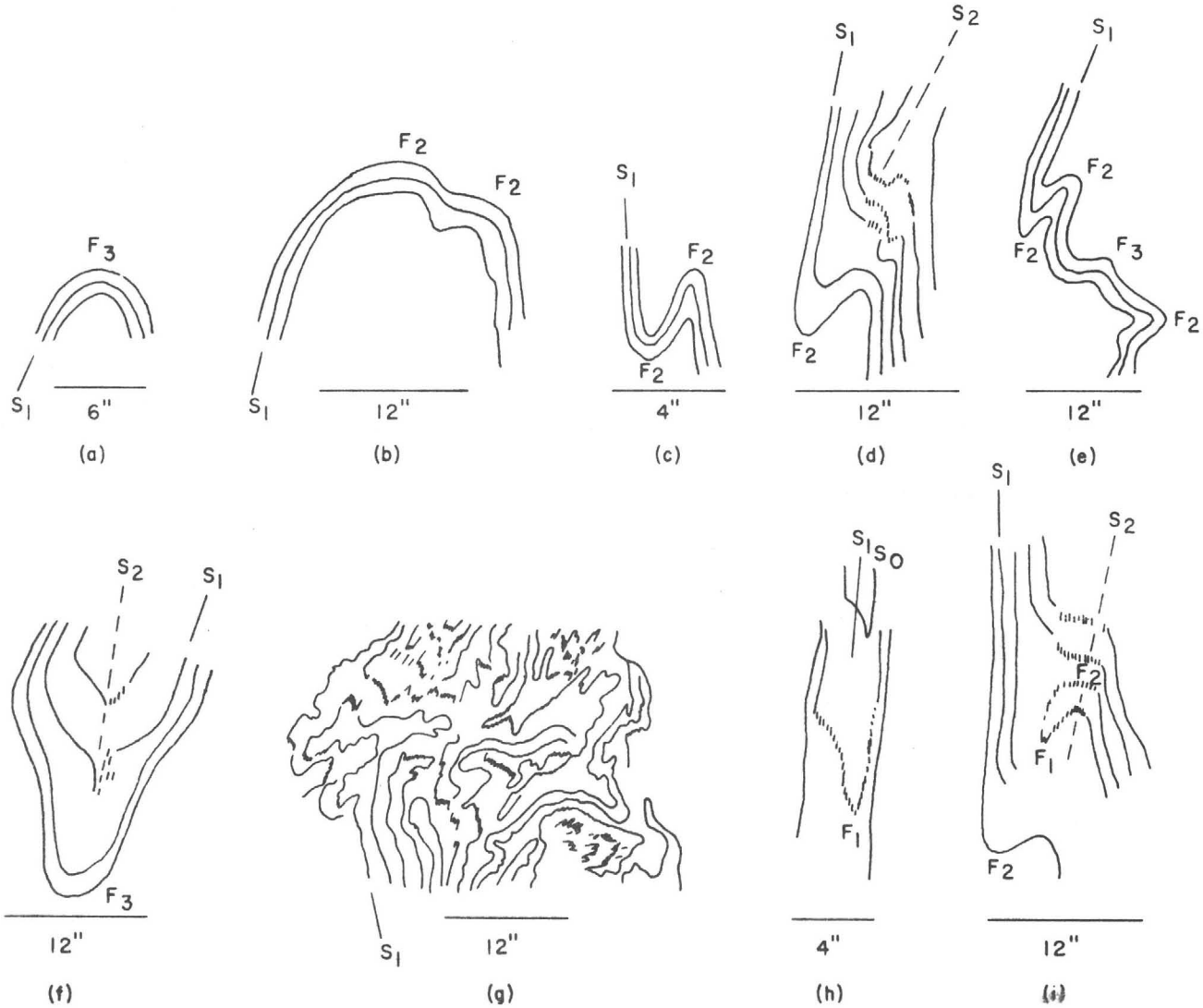

Figure 7.—Sketches of mesoscopic folds in quartzofeldspathic gneiss. All sections (except *c*, *g*, and *i*, which show non-coaxial, multiphase folding) are normal to the fold axis and are viewed down-plunge. See text for further explanation.

although schistosity in biotite schist is truncated locally at the contact. Some contact surfaces show Gleitbrett-style folding, cataclastic foliation paralleling the axial planes of the folds.

Other planar structures include closely spaced *surfaces of slickenside striae*, which correspond in attitude to foliation surfaces, and are also present locally in the "non-cataclastic interior", *microfaults* (Pl. 4, fig. 3), and *joints*, most of which parallel foliation, but some locally assume high-angle strike joint orientation.

LINEATIONS

Lineations are defined by *mineral parallelism* (feldspar augen, mica streaks, and quartz rods) and *slickenside striae.* All such lineations are oriented in the foliation planes.

BIOTITE AND QUARTZ ORIENTATION

Microscopic subfabric analyses of biotite (001) and quartz [0001] in eleven batholith samples will be re-

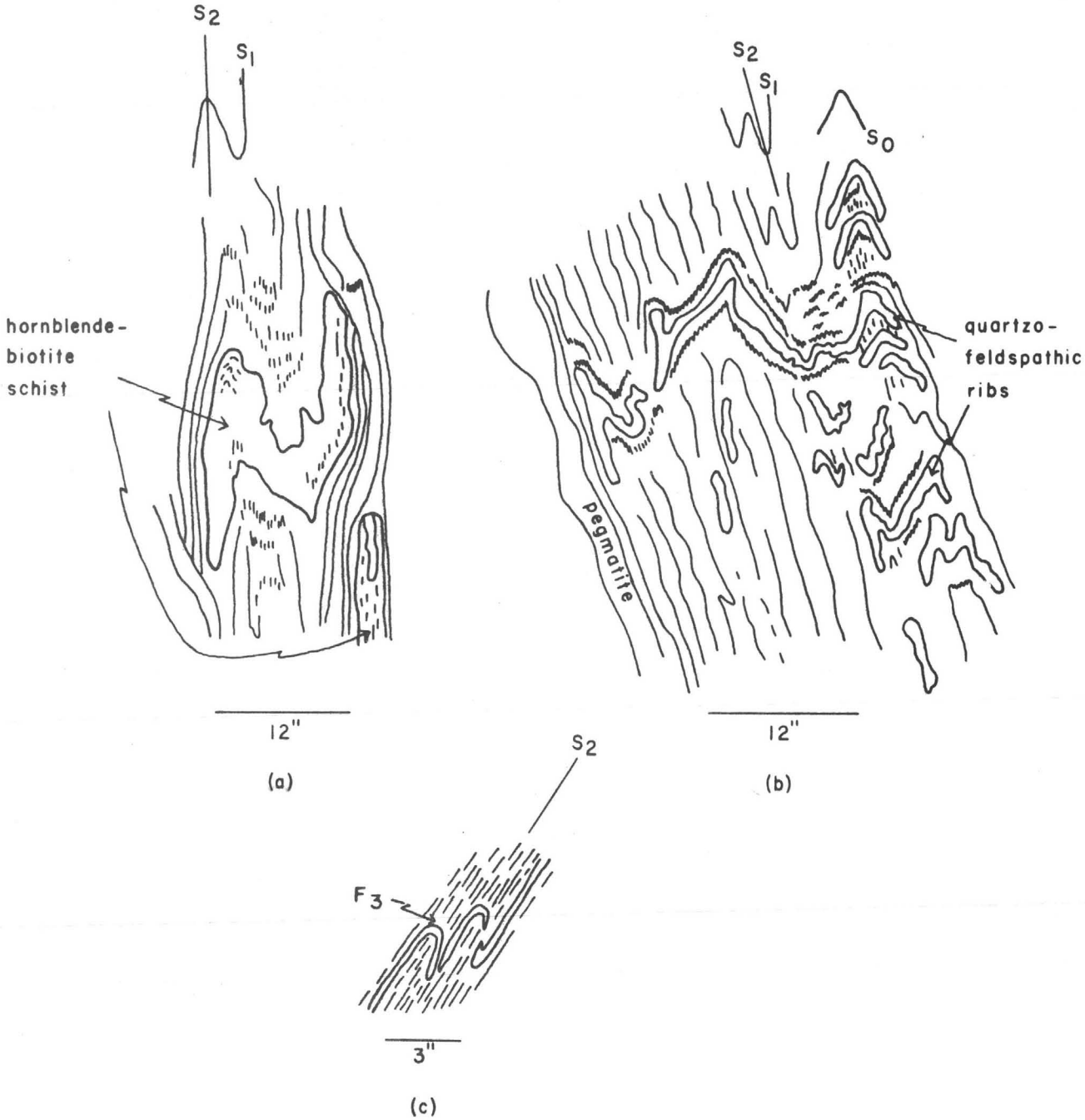

Figure 8.--Sketches of mesoscopic folds in pelitic schist. Sections *b* and *c* are normal to the fold axis and are viewed down-plunge. Section *a* shows folds which are not coaxial. See text for further explanation.

ported in a future publication, but several comments concerning subfabric distributions are warranted here.

Within the cataclastic eastern sector of the Idaho batholith, poles to biotite (001) plot in partial great-circle girdles, a reflection of wrapping of schistosity around the feldspar augen. Quartz [0001] plots as diffuse maxima bisected symmetrically by foliation and normal to mineral streak lineation. The preferred orientation of these minerals is evident within the cataclastic belt along the eastern front of the Bitterroot Range and has been reported (but not documented by petrofabric analyses in the paragneiss of Kootenai Creek Canyon (Groff, 1954), Bass and Sweeney Creek Canyons (Anderson, 1959a, p. 13-19), and south of Lolo Creek (Wehrenberg, 1968). (See Fig. 1 for localities.)

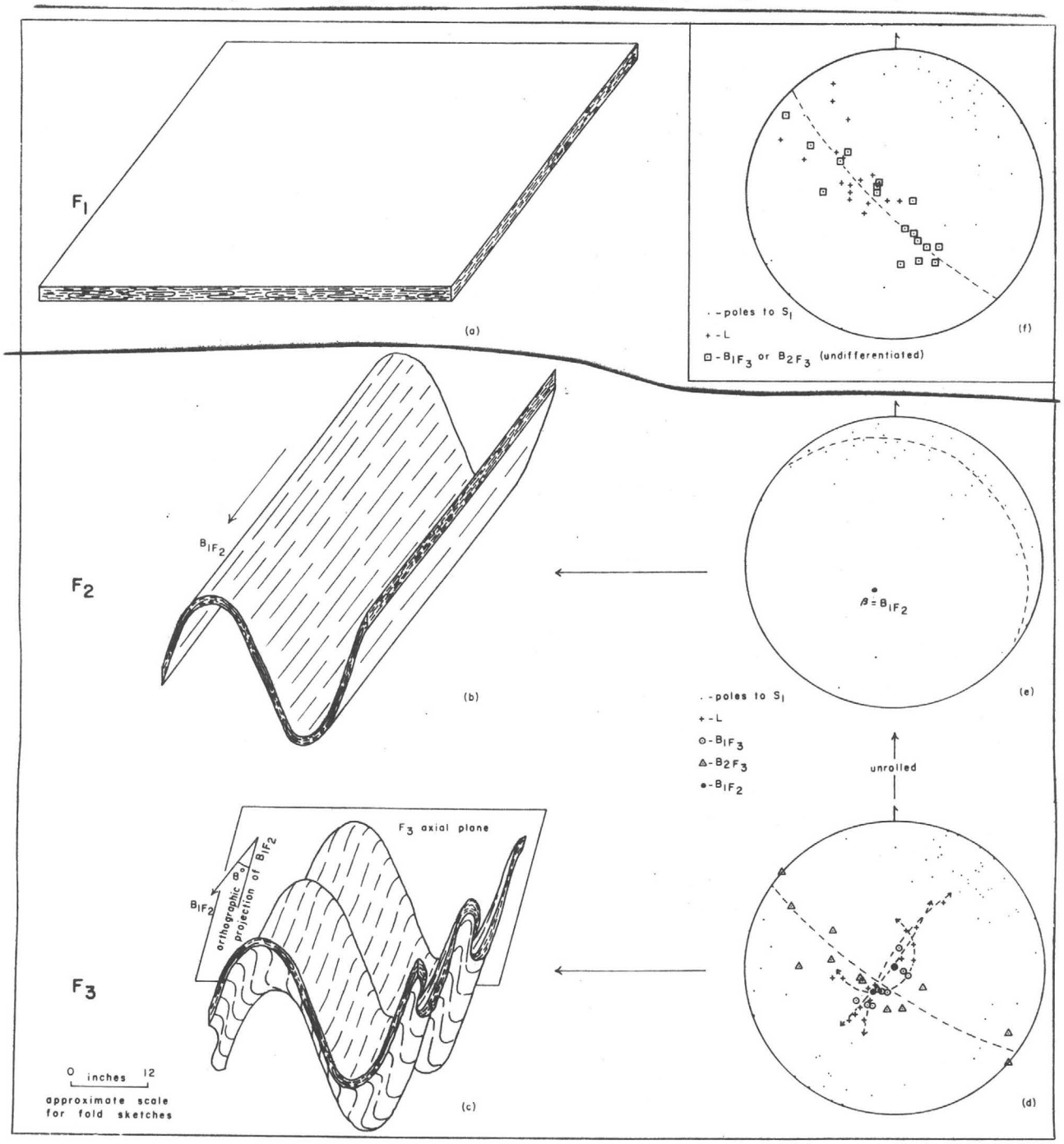

Figure 9.–*a, b,* and *c*: schematic representation of F_1, F_2, F_3 fold phases in a single outcrop of quartzofeldspathic gneiss; *d*: structural data from composites of three separate domains near South Kootenai Lake; *e*: F_3 unrolled from *d*; *f*: structural data from pelitic schist cropping out approximately 1,000 yards from the outcrop represented in *d*. Arrows on stereograms denote true north. Great and small circles represent best visual fit of data analyzed in outcrop. See text for further explanation.

In the contact zone of the batholith west of the cataclastic belt, features of cataclasis are absent, biotite (001) is unoriented or nearly planar in foliate zones, and quartz [0001] is unoriented. Thus, it is evident that the cataclastic belt is a result of a late syn- or post-intrusion structural event, the effects of which were concentrated mainly along the Bitterroot Range front.

STRUCTURAL AND METAMORPHIC HISTORY

On the basis of data gathered for this report, a structural interpretation involving five phases of folding is postulated.

F_1 folding.—In some parts of the study area, a distinct parallelism of mica schistosity and lithologic contacts between pelitic, quartzofeldspathic, and calc-silicate units was observed. This relationship of folia to contacts is indicative of development of the folia parallel to sedimentary bedding surfaces, which perhaps were accentuated by metamorphic differentiation. Two schools of thought exist concerning the origin of schistosity parallel to bedding: (1) schistosity developed by indirect componental movement ("Riecke principle" growth of minerals under the influence of load metamorphism) and (2) schistosity developed by a combination of direct and indirect componental movement (recrystallization or neocrystallization within planes of mechanical anisotropy). The concept of load metamorphism alone leading to the development of schistosity has been virtually discarded by recent workers in structural analysis. Indeed, many examples of schistosity paralleling layering on the limbs of isoclinal folds but truncating layering in the noses of these folds are cited in the literature. Examples of a schistosity-layering relationship as developed by direct componental movement have been cited in such metamorphic areas as the Shuswap Terrane, British Columbia (Jones, 1959, p. 58; Hyndman, 1968, p. 576-579), northern Vermont (Woodland, 1965, p. 67), and the Moine and Dalradian belts of the Scottish Highlands (King and Rast, 1956, p. 245). Within the study area, local similar-style folds with large amplitude/wave length ratios (Fig. 7h), some of which are refolded by F_2 deformation (Fig. 7i), suggest F_1 structures as illustrated in Figure 9a. The relationship of schistosity to lithologic contacts, however, was not examined in sufficient detail to say whether some schistosity assumes an axial-surface orientation in large-scale recumbent folds.

F_2 folding.—Second-generation structures are best observed in the quartzofeldspathic gneiss. The movement picture is one of flexural slip and concomitant development of coaxial crinkle lineation (L parallel to B_1), the preservation of most mica schistosity parallel to lithologic layering around the noses of folds (S_1), and local development of axial-plane schistosity (S_2). This geometry is reconstructed in Figures 9b and 9e. Knill (1960a, p. 350; 1960b, p. 323) has suggested that bedding schistosity can be produced during flexural slip deformation. Schistosity in much of the quartzofeldspathic gneiss is best defined along mica-rich layers, which probably served as surfaces of slip. Schistosity in the intervening quartzitic layers is not well defined, but there is sufficient preferred orientation of micas in the more feldspathic layers to indicate that deformation was penetrative during the initiation of schistosity. It is therefore thought likely that the schistosity developed prior to F_2 folding.

F_3 folding.—The third-generation folding in quartzofeldspathic gneiss is expressed by flexural slip deformation of F_2 folds and local development of incipient axial-plane schistosity. The intersection of the F_3 fold axial surfaces and S_1 surfaces of F_2 folds is represented by a great-circle girdle of B_2 lineations. L (and B_1 paralleling L) plots on small-circle girdles, which intersect at the position of the F_2 fold axis (Fig. 9c, data in Fig. 9d). All measured structural data for the pelitic schist plot in F_3 fold positions, suggesting that the F_2 form surface within the pelitic unit was destroyed by F_3 deformation (Fig. 9f). The contrasting structural styles of the paragneiss and metatonalite are striking. Whereas complex structures pervade the paragneiss, lineation and foliation in the orthogneissic unit display a constant orientation on the mesoscopic scale (Pl. 3, fig. 2). These differing structural styles suggest that the metatonalite was subjected to only one phase of penetrative deformation. This is possible if the emplacement of the tonalite was post-F_2, but pre- or syn-F_3, with synkinematic metamorphism. It is unlikely that F_2 structures could be destroyed in quartzofeldspathic metatonalite and remain preserved in an adjacent quartzofeldspathic gneiss.

A partial metamorphic paragenesis is postulated with consideration of the following:

(1) The production of mica schistosity requires metamorphic conditions of at least biotite grade. The few grains of garnet observed in some samples show no internal fabric or helicitic structure. Thus, the growth of these garnets probably preceded the development of the mica subfabric (Zwart, 1960, fig. 4). The sillimanite subfabric is attributed to replacement of, or epitaxial growth on, biotite. Thus, sillimanite could have formed during the development of the mica subfabric, but need not have. The metamorphic conditions, therefore, were above biotite grade (locally garnet grade) and could have reached sillimanite grade during F_1 folding.

(2) The sillimanite that outlines the noses of preexisting crenulations crystallized prior to the transposition of foliation (F_3 in pelitic schist). Metamorphism, therefore, reached conditions of sillimanite grade prior to or during the incipient stage of F_3 folding.

F_4 folding.—The close conformity of macroscopic structural patterns to the curving border of the Idaho batholith and its apophyses (Pl. 1) suggests an intrusive influence on present paragneissic structures. A subarea analysis of mesoscopic structures in the contact zone emphasizes this structural conformity.* It is possible that this broad, macroscopic flexural pattern either (1) predated intrusion of the Idaho batholith, effecting a selective migration of quartz monzonitic-granodioritic magma into warped planes of structural anisotropy, (2) was produced by forces generated by intrusion, (3) is a post-intrusion event, or (4) is associated with two or all three of the above possibilities in the same event.

The formation of polygonal arcs in mica crenulations and the de-orientation of quartz were probably effected by a thermal event associated with batholithic intrusion and perhaps with F_4 folding. Recrystallization was at least biotite grade. The lack of a contact metamorphic mineral suite suggests that this thermal pulse occurred prior to significant cooling after the peak of regional metamorphism.

There is no evidence to suggest anything other than one phase of regional metamorphism associated with multiphase deformation. On the basis of similar textural evidence in an equally complex structural area within the Scottish Highlands, Harte and Johnson (1969) presented the same conclusion.

F_5 deformation.—The cataclastic deformation of the Idaho batholith (and the metasedimentary units in the northern Bitterroot Range) and Gleitbrett-style folding of biotite gneiss layers and pegmatite along the eastern front of the Bitterroot Range represent the final penetrative deformation in the study area. This deformation may be the result of a broad macroscopic flexure or of diapiric uplift along a north-trending axis (the latter suggested by Reesor, 1965, p. 120, for the east flank of the Valhalla and Passmore domes, British Columbia).

CONCLUSIONS

Pelitic, quartzofeldspathic, and calcareous sediments probably of the Belt Supergroup (Precambrian) have been regionally metamorphosed adjacent to the northeastern border of the Idaho batholith. The paragneiss contains concordant amphibolite pods and anorthosite bodies, and displays mineral assemblages (with some disequilibrium textures) characteristic of sillimanite-potassium feldspar-grade or, locally, sillimanite-muscovite-grade metamorphism.

Penetrative deformation involved a proposed first phase, F_1, which produced a mica schistosity paralleling lithologic layers (probably original beds). F_1 is suggested by the strong parallelism of schistosity and layering and high amplitude/wave length ratios of some folds. A second deformation, F_2, resulted in flexural slip folding of lithologic layers and mica schistosity and associated development of mica crinkle lineation (paralleling F_2 fold axes) and incipient axial-plane schistosity. A third deformation, F_3, produced the small-circle rotation of F_2 fold axes and mica crinkles, and the superposition of mesoscopic F_3 folds on existing F_2 folds in the quartzofeldspathic gneiss. The concomitant development of crenulation foliation and axial-plane mica schistosity nearly obliterated F_2 structures in the pelitic schist. Calc-silicate layers and amphibolite bodies were stretched into boudins during one of the penetrative deformations. Synkinematic to deformation was regional metamorphism, the anatectic production of pegmatite veins, and the emplacement of a tonalite stock in the quartzofeldspathic gneiss.

Emplacement of Idaho batholith quartz monzonite-granodiorite and associated apophyses, pegmatite, and aplite postdates the penetrative deformations and the peak of regional metamorphism. A contact breccia of batholithic rock and calc-silicate gneiss, rotation of structural subareas (F_4 deformation) adjacent to the batholith, and the gradational contact between the batholith and quartzofeldspathic gneiss suggest plutonic activity involving a complex interplay of magmatic stoping, forceful intrusion, and contact metasomatism. Subsolidus adjustments during the pluton evolution include the growth of potassium feldspar megacrysts, development of albite rims on plagioclase at microperthite-plagioclase interfaces, and the growth of myrmekitic plagioclase adjacent to potassium feldspar. Irregular foliate zones in the pluton are the result of primary flow, cataclastic deformation, or inheritance of foliation from incompletely assimilated quartzofeldspathic xenoliths, each factor accounting for some such segments of the pluton. Tonalite in the batholith border zone conceivably resulted from contamination of quartz monzonite-granodiorite

*This subarea analysis will be discussed in a future publication.

magma by chemical components from calc-silicate xenoliths. Dip of schistosity in metasediments under the batholith and the topographic expression of the contact suggest the floor of a sheetlike pluton.

Thermal recrystallization of quartz and micas accompanied Idaho batholith emplacement, but the mineral assemblages formed during regional metamorphism were in large part stable in the temperature-pressure field of igneous activity. This suggests that the batholith was emplaced prior to significant cooling after the peak of regional metamorphism.

Cataclastic flowage (F_5 deformation) within a segment of the Idaho batholith associated with the eastern front of the Bitterroot Range postdates batholithic emplacement and consolidation, but did not affect earlier formed structures in the core of the range.

POSSIBLE ECONOMIC IMPLICATIONS

The lack of economically significant mineralization associated with the Idaho batholith in the Bitterroot Range has long been a geologic puzzle. Only the lead-zinc-silver-producing Curlew mine, at the mouth of Big Creek, 3 miles east of the study area, has any history of production in the last 50 years (Sahinen, 1957, p. 18). Within the study area, investigation of the Starr mine, at the junction of Big Creek and its North Fork, revealed a 15-foot adit into a barren zone at the contact of pelitic schist and a quartz monzonite dike.

Topographic and structural evidence has been presented to suggest that the Idaho batholith is a sheetlike pluton and that its base was mapped in the study area. If any mineralization associated with the main massif of the batholith were hydrothermal in origin and accomplished by ascending solutions or lateral secretion, post-intrusion erosion would have since removed such deposits. Thus, the lack of significant mineralization in the Bitterroot Range could be attributed directly to the depth of the present erosion level.

REFERENCES CITED

ANDERSON, R. E., 1959, Genesis of anorthosite bodies within the metamorphic rocks of the Bitterroot Range, Montana [abs.]: Geol. Soc. America Bull., v. 70, p. 1773.

———1959a, Geology of lower Bass Creek canyon, Bitterroot Range, Montana: M.S. thesis, Univ. of Montana, 70 p.

BARTH, T. F. W., 1956, Zonal structure in feldspars of crystalline schists, *in* Trabajos de la Tercera Reunion Internacional sobre Reactividad do los Solidos, v. 2, p. 365-371.

BERG, R. B., 1964, Petrology of anorthosite bodies, Bitterroot Range, Ravalli County, Montana: Ph.D. thesis, Univ. of Montana, 158 p.

———1965, Petrology of anorthosite bodies in the Bitterroot Range, western Montana [abs.]: Geol. Soc. America Spec. Paper 82, Abstracts for 1964, p. 319.

CHASE, R. B., 1961, Geology of lower Sweathouse Creek canyon, Bitterroot Range, Ravalli County, Montana: M.S. thesis, Univ. of Montana, 83 p.

———1965, Border-zone petrology of the Idaho batholith within a portion of western Montana [abs.]: Geol. Soc. America Spec. Paper 82, Abstracts for 1964, p. 323.

———1968, Regional metamorphism adjacent to the northeastern portion of the Idaho batholith [abs.]: Geol. Soc. America Spec. Paper 115, Abstracts for 1967, p. 412.

DEER, W. A., HOWIE, P. A., and ZUSSMAN, J., 1962a, Rock forming minerals, v. 1: New York, John Wiley and Sons, Inc., 333 p.

———1962b, Rock forming minerals, v. 3: New York, John Wiley and Sons, Inc., 270 p.

———1963, Rock forming minerals, v. 2: New York, John Wiley and Sons, Inc., 379 p.

EMMERMANN, Rolf, 1969, Genetic relations between two generations of K-feldspar in a granite pluton: N. Jb. Miner. Abh., v. 111, no. 3, p. 289-313.

EVANS, B. W., and GUIDOTTI, C. V., 1966, The sillimanite-potash feldspar isograd in western Maine, U. S. A.: Contr. Mineralogy and Petrology, v. 12, p. 25-62.

GIBSON, Russell, 1948, Geology and ore deposits of the Libby quadrangle, Montana: U. S. Geol. Survey Bull. 956, 131 p.

GROFF, S. L., 1954, Petrology of a portion of the eastern front of the Bitterroot Range, Montana [abs.]: Geol. Soc. America Bull., v. 65, p. 1376.

———1954a, Petrography of the Kootenai Creek area, Bitterroot Range, Montana: M.A. thesis, Univ. of Montana, 80 p.

GUIDOTTI, C. V., 1963, Metamorphism of the pelitic schists in the Bryant Pond quadrangle, Maine: Am. Mineralogist, v. 48, p. 772-791.

HARTE, B., and JOHNSON, M. R. W., 1969, Metamorphic history of Dalradian rocks in Glens Clova, Esk and Lethnot, Angus, Scotland: Scottish Jour. Geol., v. 5, no. 1, p. 54-80.

HOBBS, S. W., GRIGGS, A. B., WALLACE, R. E., and CAMPBELL, A. B., 1965, Geology of the Coeur d'Alene district, Shoshone County, Idaho: U. S. Geol. Survey Prof. Paper 478, 139 p.

HYNDMAN, D. W., 1968, Mid-Mesozoic multiphase folding along the border of the Shuswap metamorphic complex: Geol. Soc. America Bull., v. 79, p. 575-588.

———, ALT, W. D., and NOLD, J. L., 1968, Some limits to diffusion during regional metamorphism north of the Idaho batholith [abs.]: Geol. Soc. America Spec. Paper 115, Abstracts for 1967, p. 106.

JONES, A. G., 1959, Vernon map area, British Columbia: Canada Geol. Survey Mem. 296, 186 p.

KING, B. C., and RAST, Nicholas, 1956, Tectonic styles in the Dalradian and Moines of parts of the central Highlands of Scotland: Geol. Assoc. Proc., v. 66 (for 1955), p. 243-269.

KNILL, J. L., 1960a, The tectonic pattern in the Dalradian of the Craignish-Kilmelfort district, Argyllshire: Geol. Soc. London Quart. Jour., v. 115 (for 1959), p. 339-364.

-----1960b, A classification of cleavages, with special references to the Craignish district of the Scottish Highlands: Internat. Geol. Cong., 21st, Copenhagen, pt. 18, p. 317-325.

LANGTON, C. M., 1935, Geology of the northeastern part of the Idaho batholith and adjacent region in Montana: Jour. Geology, v. 43, p. 27-60.

LARSEN, E. S., Jr., and SCHMIDT, R. G., 1958, A reconnaissance of the Idaho batholith and comparison with the southern California batholith: U. S. Geol. Survey Bull. 1070-A, p. 1-32.

LINDGREN, Waldemar, 1904, A geological reconnaissance across the Bitterroot Range and Clearwater Mountains in Montana and Idaho: U. S. Geol. Survey Prof. Paper 27, 123 p.

LUTH, W. C., JAHNS, R. H., and TUTTLE, O. F., 1964, The granite system at pressures of 4 to 10 kilobars: Jour. Geophys. Research, v. 69, no. 4, p. 759-773.

NEWTON, R. C., 1966, Kyanite-andalusite equilibrium from 700° to 800°C: Science, v. 153, p. 170-172.

NOLD, J. L., 1968, Geology of the northeastern border zone of the Idaho batholith, Montana and Idaho: Ph.D. thesis, Univ. of Montana, 159 p.

-----1969, Relation of regional metamorphism to igneous rocks–northeast border zone of the Idaho batholith [abs.]: Geol. Soc. America Spec. Paper 121, Abstracts for 1968, p. 618.

ORVILLE, P. M., 1962, Alkali metasomatism and feldspars: Norsk geol. tidsskr., v. 42 supp. (Feldspar Volume), p. 283-316.

-----1963, Alkali ion exchange between vapor and feldspar phases: Am. Jour. Sci., v. 261, p. 201-237.

REESOR, J. E., 1965, Structural evolution and plutonism in Valhalla gneiss complex, British Columbia: Canada Geol. Survey Bull. 129, 128 p.

ROSS, C. P., 1950, The eastern front of the Bitterroot Range, Montana: U. S. Geol. Survey Bull. 974-E, p. 135-175.

-----1963, The Belt Series in Montana: U. S. Geol. Survey Prof. Paper 346, 122 p.

SAHINEN, U. M., 1957, Mines and mineral deposits, Missoula and Ravalli Counties, Montana: Montana Bur. Mines and Geol. Bull. 8, 63 p.

TURNER, F. J., and WEISS, L. E., 1963, Structural analysis of metamorphic tectonites: New York, McGraw-Hill Book Co., 545 p.

TUTTLE, O. F., 1952, Origin of contrasting mineralogy of extrusive and plutonic salic rocks: Jour. Geology, v. 60, p. 107-124.

-----, and BOWEN, N. L., 1958, Origin of granite in the light of experimental studies in the system $NaAlSi_3O_8-KAlSi_3O_8-SiO_2-H_2O$: Geol. Soc. America Mem. 74, 153 p.

VELDE, Bruce, 1965, Experimental determination of muscovite polymorph stabilities: Am. Mineralogist, v. 50, p. 436-449.

von PLATEN, Hilmar, 1965, Experimental anatexis and genesis of migmatites, p. 203-218, *in* Controls of metamorphism: Edinburgh, Oliver and Boyd, Ltd., 368 p.

WEHRENBERG, J. P., 1968, Structural development of the northern Bitterroot Range, western Montana [abs.]: Geol. Soc. America Spec. Paper 115, Abstracts for 1967, p. 456.

WEILL, D. F., 1966, Stability relations in the $Al_2O_3-SiO_2$ system calculated from solubilities in the $Al_2O_3-SiO_2-Na_3AlF_6$ system: Geochem. et Cosmochim. Acta, v. 30, p. 223-237.

WINKLER, H. G. F., 1965, Petrogenesis of metamorphic rocks: New York, Springer-Verlag New York, Inc., 220 p.

WOODLAND, B. G., 1965, The geology of the Burke quadrangle, Vermont: Vermont Geol. Survey Bull. 28, 151 p.

YODER, H. S., STEWART, D. B., and SMITH, J. R., 1957, Ternary feldspars: Carnegie Inst. Washington, Yearbook 56, p. 206-214.

ZWART, H. J., 1960, The chronological succession of folding and metamorphism in the central Pyrennes: Geol. Rundschau., v. 50, p. 203-218.

EXPLANATION OF PHOTOGRAPHS

PLATE 2

Fig. 1.—Typical pelitic schist illustrating the fine lithologic layering and small-scale, concentric-style folds which represent incipient development of crenulation foliation (strain-slip cleavage).

Fig. 2.—Similar-style folds outlined by leucocratic layers in pelitic schist.

Fig. 3.—Non-bent cleavage flakes of biotite which outline the apex of a tight similar-style fold in pelitic schist. Analyzer out.

Fig. 4.—Ptygmatic-style folds in pegmatite within quartzofeldspathic gneiss. Estimated mode of pegmatite plus mafic selvages (bordering pegmatite) approximately equals mode of quartzofeldspathic gneiss.

PLATE 3

Fig. 1.—Lithologic layering in calc-silicate gneiss. Black—hornblende, gray—diopside, white—mosaic of plagioclase and quartz.

Fig. 2.—Deformed and metamorphosed, zoned (biotite-rich core) pegmatite in metatonalite. Axial plane biotite schistosity in pegmatite parallels biotite schistosity and schlieren (straight streaks) in host tonalite.

Fig. 3.—Hypidiomorphic-granular granodiorite of the Idaho batholith. Analyzer in.

Fig. 4.—Mineral and rock fragment inclusions in microcline megacryst within the Idaho batholith. Analyzer in.

PLATE 4

Fig. 1.—Hypidiomorphic-granular quartz monzonite of the Idaho batholith containing microcline microperthite megacrysts. The finer-grained matrix is predominantly biotite, quartz, and plagioclase.

Fig. 2.—Specimen from the zone of strong cataclasis of the Idaho batholith. The foliation is defined by segregated layers (locally wrapped around feldspar augen) of granulated quartz, granulated feldspar, and uncrushed rock.

Fig. 3.—Mosaic texture of specimen from the zone of strong cataclasis of the Idaho batholith. Crush layers are offset by a microfault. Analyzer in.

Fig. 4.—Contact breccia area of the Idaho batholith border where isotropic tonalite contains closely-spaced calc-silicate gneiss xenoliths.

PLATE 5

Fig. 1.—Contact zone of the Idaho batholith and quartzofeldspathic gneiss. Sill-like sheets of isotropic granodiorite (containing zoned plagioclase) are intermixed with gneissic folia, resulting in a grossly gradational contact.

Fig. 2.—Metatonalite xenolith displaying biotite schlieren (dark stringers) and pegmatite enclosed in a potassium feldspar megacryst-bearing apophysis of the Idaho batholith. Shadows across the outcrop (normal to the fracture) outline relief from glacial abrasion.

Fig. 3.—Mineral assemblage considered as A_3 in which "clean" muscovite (white cleavage flakes in center) and inclusion-free, undulose quartz with polygonal borders (upper right) are associated with biotite-sillimanite overgrowths (small gray cleavage flakes and needles in center), "clean" biotite (larger gray to black cleavage flakes in center), and orthoclase microperthite (large grain in lower right). The orthoclase is part of a coarse-grained, composite quartz-feldspar lens. Analyzer in.

Fig. 4.—Mineral assemblage considered as A_4 in which "ragged" muscovite is largely replaced by fibrolitic sillimanite (center) in association with "clean" biotite (dark gray to black cleavage flakes), embayed quartz containing sillimanite needles (white grain in right center) and orthoclase (light gray grains along lower edge). The orthoclase is part of the schistose texture. Analyzer in.

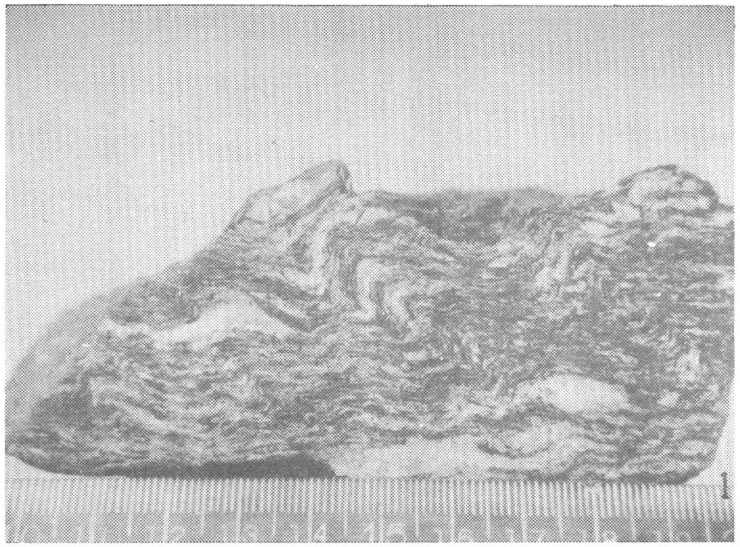

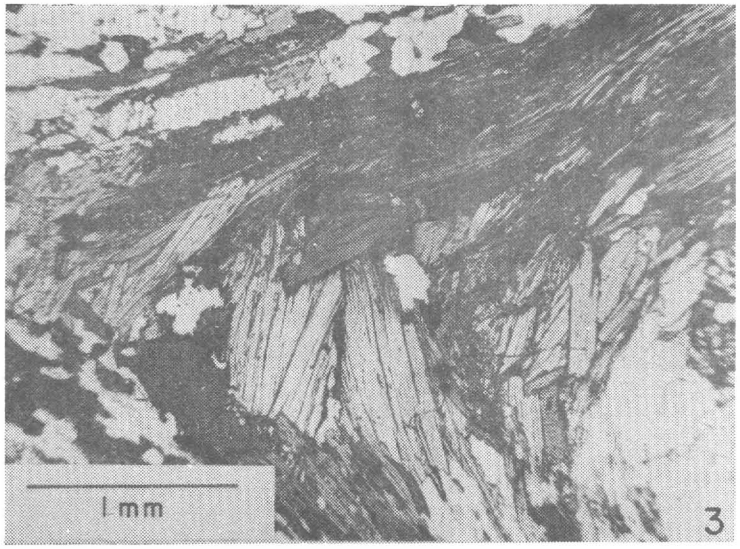

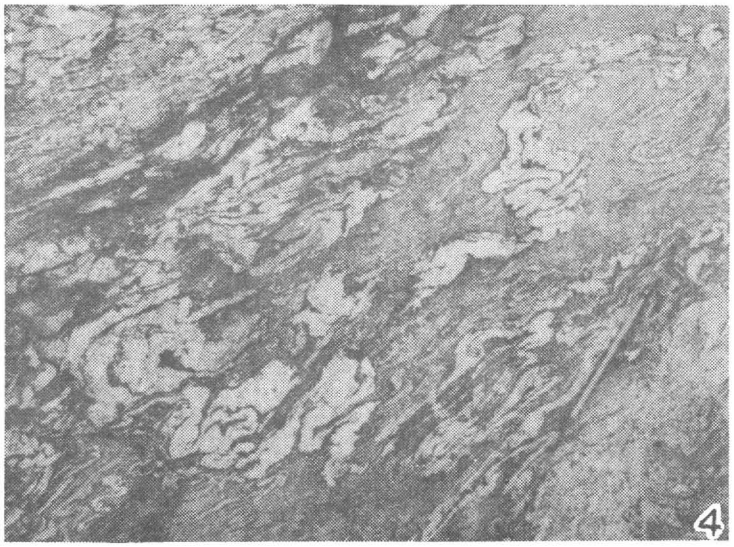

Plate 2

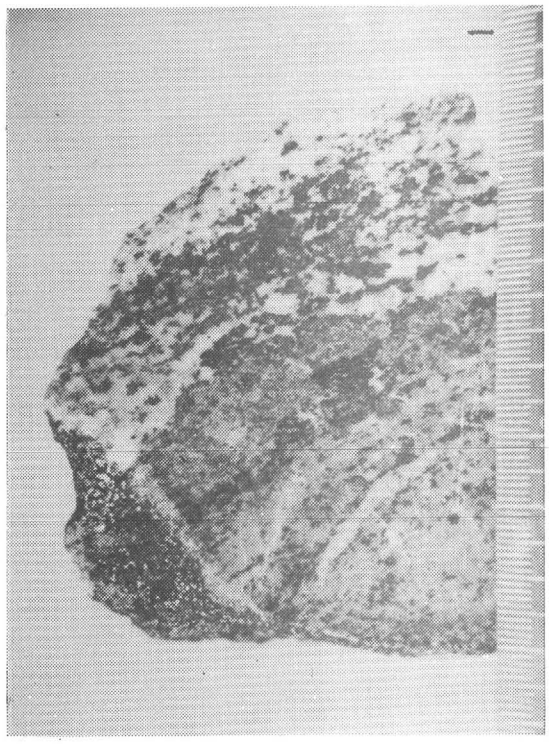

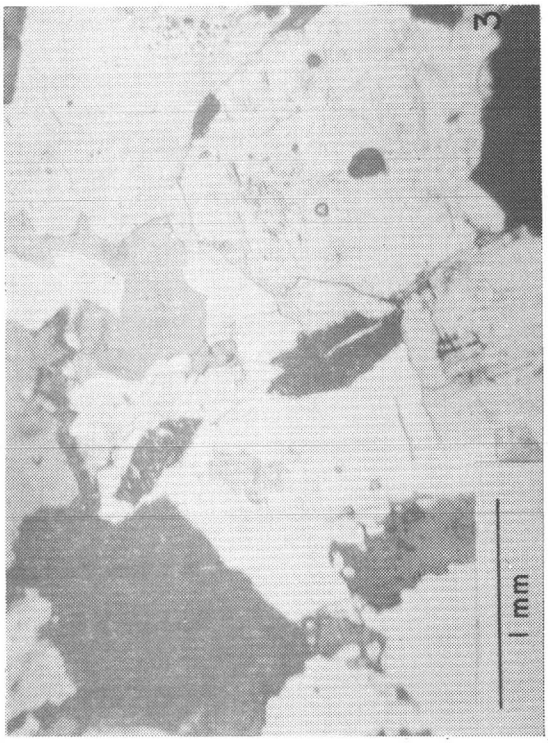

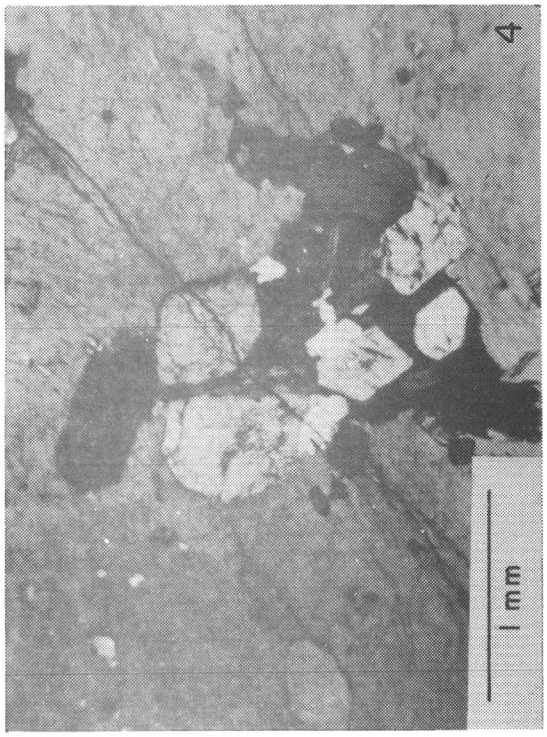

Plate 3

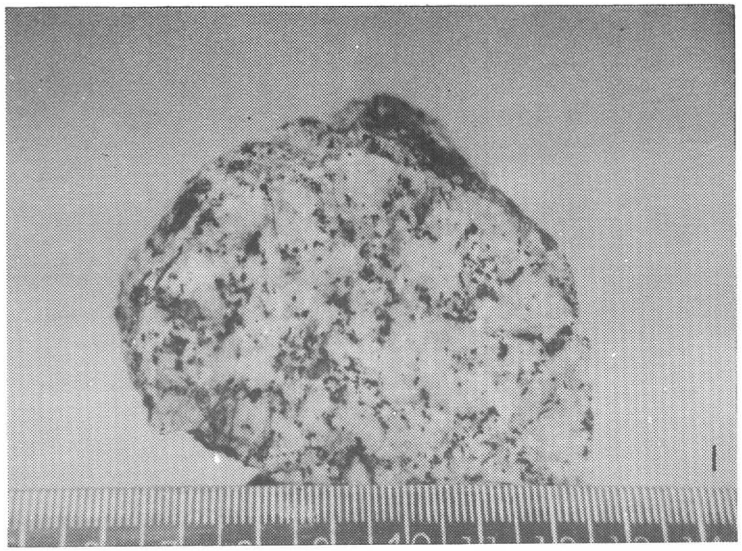

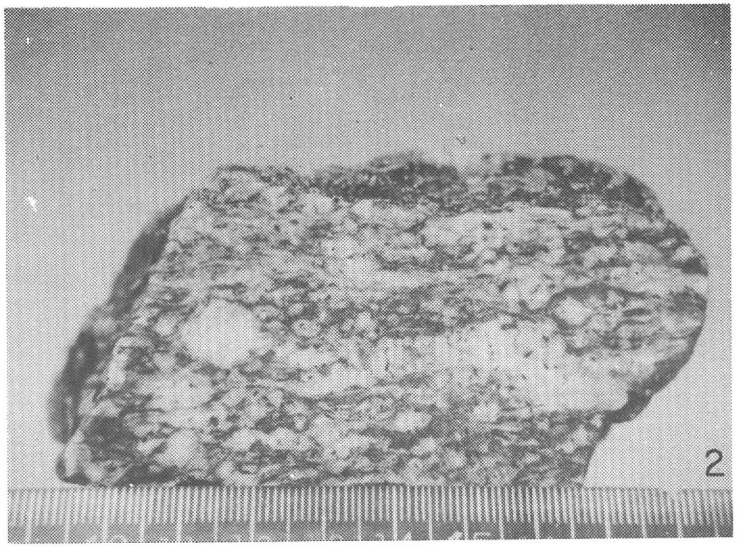

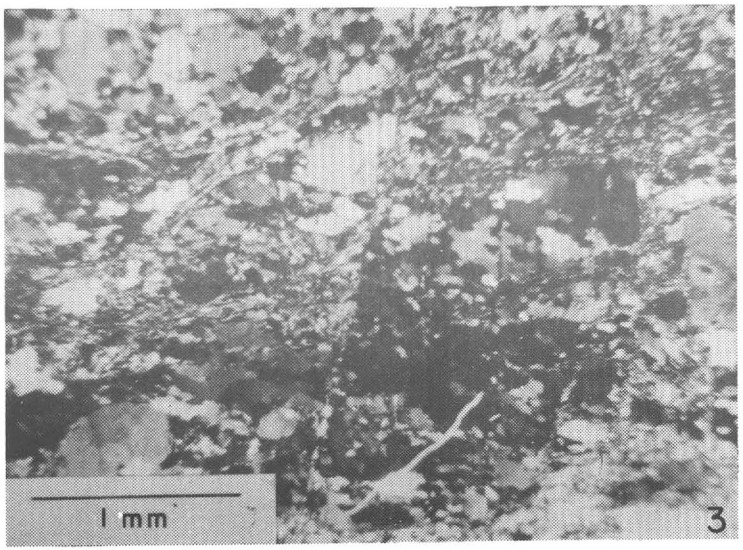

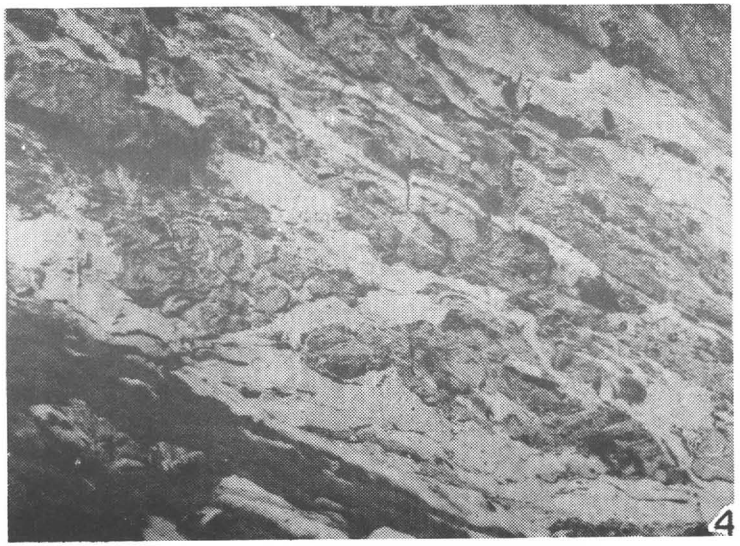

Plate 4

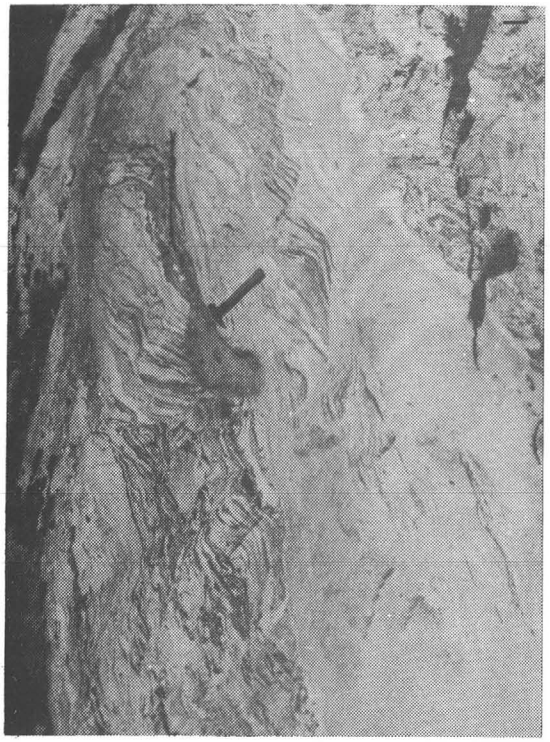

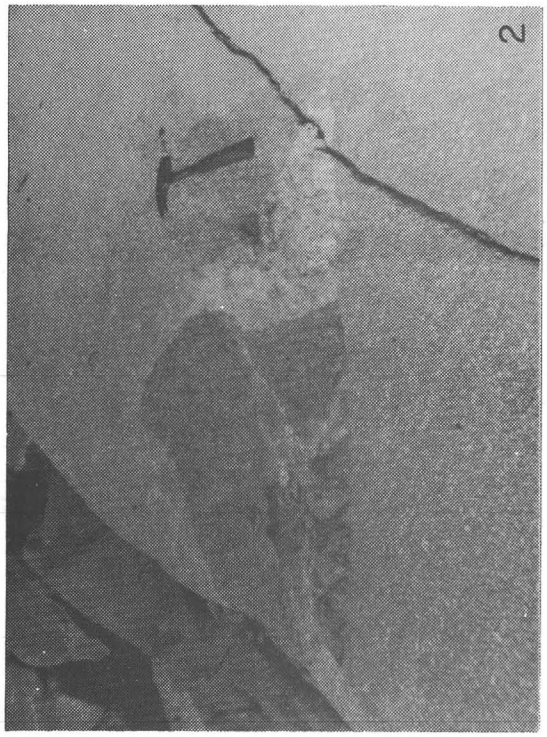

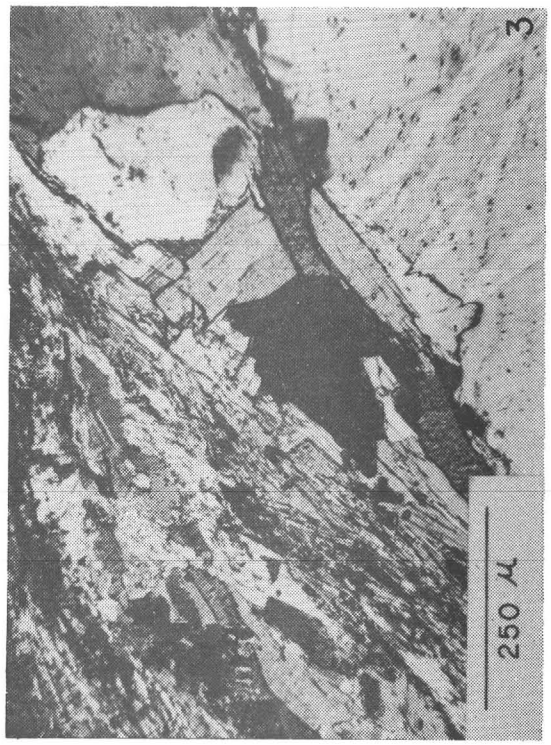

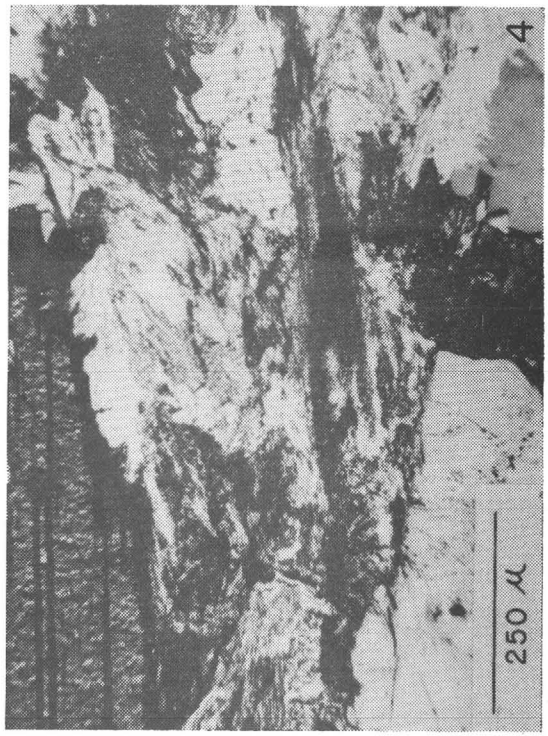

Plate 5

THE MONTANA BUREAU OF MINES AND GEOLOGY IS A PUBLIC SERVICE AGENCY FOR THE STATE OF MONTANA. ITS PURPOSE IS TO ASSIST IN DEVELOPING THE STATE'S MINERAL RESOURCES. IT CONDUCTS FIELD STUDIES OF MONTANA GEOLOGY AND MINERAL DEPOSITS, INCLUDING METALS, OIL AND GAS, COAL, AND OTHER NONMETALLIC MINERALS, AND GROUND WATER. IT ALSO CARRIES OUT RESEARCH IN MINERAL BENEFICIATION, EXTRACTIVE METALLURGY, AND ECONOMIC PROBLEMS CONNECTED WITH THE MINERAL INDUSTRY IN MONTANA. THE RESULTS OF THESE STUDIES ARE PUBLISHED IN REPORTS SUCH AS THIS.

FOR FURTHER INFORMATION, ADDRESS THE DIRECTOR, MONTANA BUREAU OF MINES AND GEOLOGY, MONTANA COLLEGE OF MINERAL SCIENCE AND TECHNOLOGY, BUTTE.

GEOLOGIC MAP AND STRUCTURE SECTIONS OF NORTHEASTERN BORDER OF IDAHO BATHOLITH, BITTERROOT RANGE, MONTANA

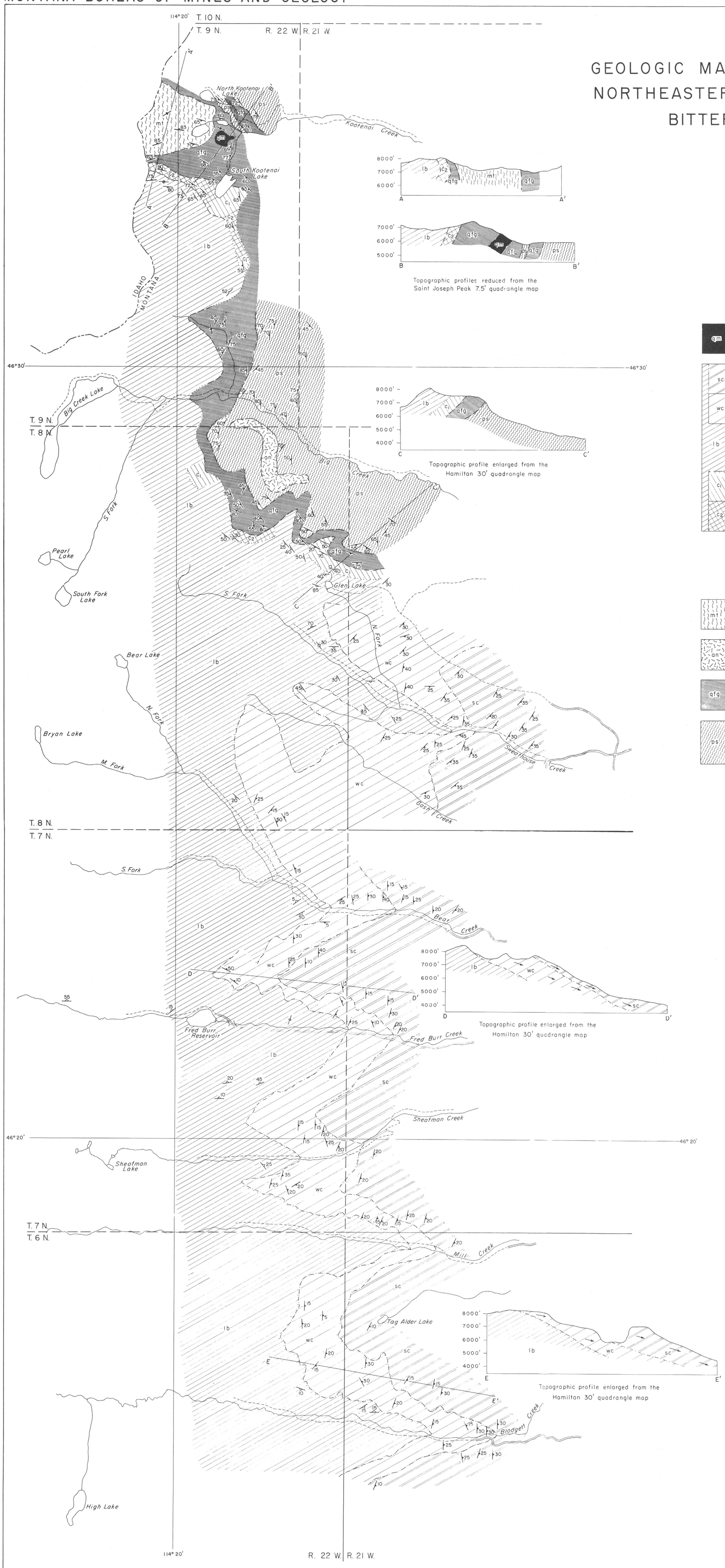

MAP EXPLANATION

IGNEOUS UNITS

Quartz monzonite: small, discordant, biotite-bearing, with allotriomorphic-granular texture and isotropic fabric

Zone of strong cataclasis: sheared augen gneiss sector of the Idaho batholith

Zone of weak cataclasis: transitional fabric area between frontal-zone augen gneiss and massive batholith rock

Idaho batholith: biotite-bearing quartz monzonite and granodiorite with dominant hypidiomorphic-granular texture and isotropic fabric; local foliate zones and fine- to medium-grained biotite gneiss inclusions irregularly distributed. Contact areas not designated c_1, or c_2 are compositionally undifferentiated

Contact zone dominantly tonalite sills and calc-silicate xenoliths

Contact zone dominantly quartz monzonite or granodiorite sills and quartzitic or quatzofeldspathic xenoliths

METAMORPHIC UNITS

Meta-tonalite: deformed and metamorphosed stock with strong biotite schistosity; contains numerous (some folded) pegmatites

Anorthosite: slightly foliated, concordant andesine to labradorite rock with associated quartz monzonite and amphibolite pods

Quartzofeldspathic gneiss: lithologically layered biotite-feldspar-quartz gneiss containing amphibolite and calc-silicate gneiss boudins and pegmatite veins

Pelitic schist: locally layered sillimanite-feldspar-biotite-quartz schist containing amphibolite, hornblende-biotite gneiss, calc-silicate gneiss, and pegmatite boudins

AREAL SYMBOLS

Road

Trail

Stream

Lithologic contacts

Exact

Approximate

Inferred

Gradational texture boundary

Structure symbols

Strike and dip of mica schistosity in distincty foliated units (vertical dip)

Strike and dip of foliation in local areas of the Idaho batholith (vertical dip)

Strike and dip of schistosity in gneissic xenoliths within the Idaho batholith (vertical dip)

Plunge of augen lineation (cross sections)

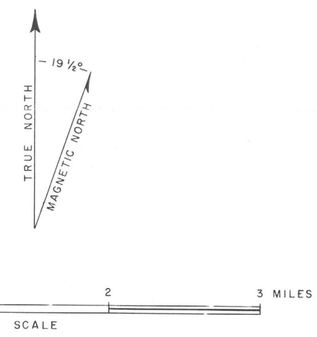

Data by Ronald B. Chase, 1960, 1962, and 1963: mapped on aerial photographs and transferred to U. S. Forest Service ridge and stream strip maps by Vertical Sketchmaster

Ronald B. Chase, 1968